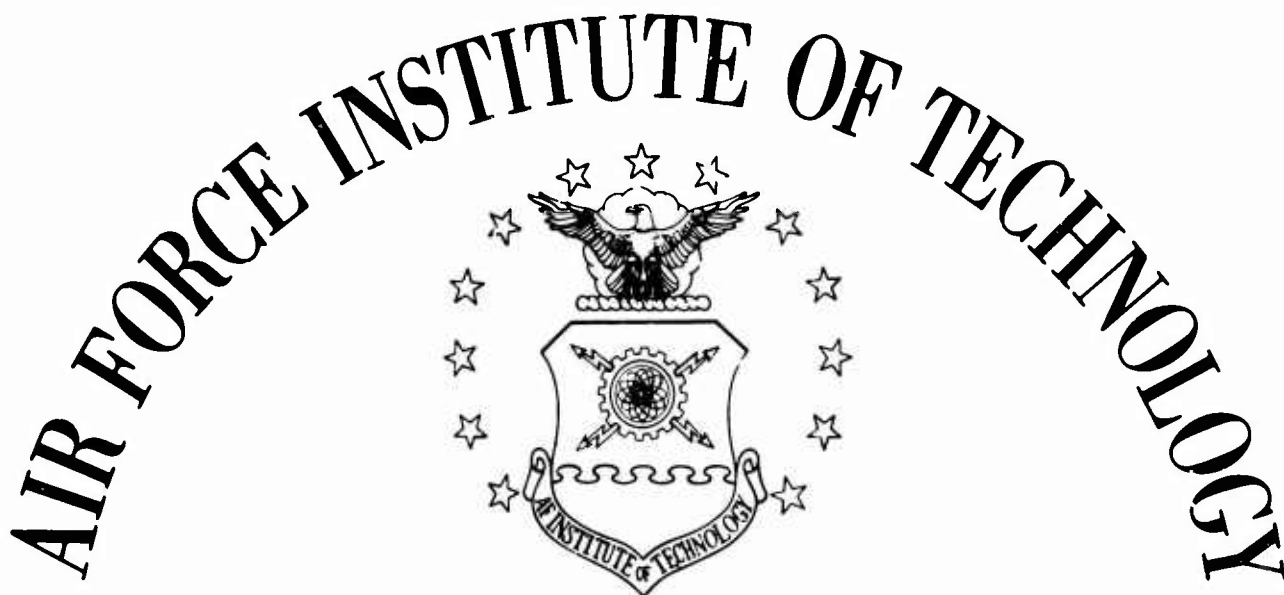


AD 642361



AIR UNIVERSITY  
UNITED STATES AIR FORCE

BUOYANT PLANETARY ENTRY

THESIS

GAM/AE/66A-2

Reginangelo A. DiPilla

Captain

USAF

CLEARINGHOUSE FOR FEDERAL SCIENTIFIC AND TECHNICAL INFORMATION	
Hardcopy	Microfiche
\$3.00	\$1.65
124 pp	
/ ARCHIVE COPY	

SCHOOL OF ENGINEERING

WRIGHT-PATTERSON AIR FORCE BASE, OHIO

DDC  
RECORDED  
NOV 28 1966  
C

BUOYANT PLANETARY ENTRY

THESIS

Presented to the Faculty of the School of Engineering of  
the Air Force Institute of Technology  
Air University  
in Partial Fulfillment of the  
Requirements for the Degree of  
Master of Science

Distribution of this  
document is unlimited

by

Reginangelo A. DiPilla, B.S.A.E.

Captain

USAF

Graduate Aerospace-Mechanical Engineering

March 1966

Preface

It would be significant if buoyant capsules could be safely entered into a planetary atmosphere. These "balloons" could float in the atmosphere for a long time and would be very useful precursors of manned planetary exploration missions. They could also be used to deliver instrument payloads in "soft" landings on planets as an alternative method to parachutes and retrorockets. The purpose of this study is to examine the effect of large buoyant volumes on the entry dynamics and heating of buoyant capsules and to look at some possible methods for accomplishing this type of planetary entry. The study is primarily concerned with entry dynamics; however, a discussion of the effect of buoyancy on entry heating, and methods of protecting against heating, is included.

I wish to express my appreciation to Captain Ronald E. Van Putte, who taught a course in re-entry dynamics when it was most needed, and whose notes were primarily used to develop the basic equations of motion. I also wish to thank Professor Peter Bielkowicz, Major Daniel W. Cheatham, and Captain Van Putte for reviewing the manuscript. Their criticism, recommendations, and advice are most gratefully appreciated. Any errors in this study are, of course, totally mine. Finally, I wish to thank Miss Marilyn Miller, librarian, whose help and assistance in obtaining research materials was beyond the mere call of duty, and Airman Ernest Jones, who drew most of the figures.

Reginangelo A. DiPilla

List of Figures

<u>Figures</u>		<u>Page</u>
1	Coordinate System for Buoyant Planetary Entry . . . . .	17
2	Moments About the Center of Gravity of an Entry Vehicle Due to the Applied Forces . . . . .	19
3	Planetary Approach Velocity Reduction and Injection of Entry Vehicle Into Circular Orbit by Atmospheric Grazing Maneuver . . . . .	45
4	Coordinate System for Terminal Descent of Buoyant Planetary Entry Vehicle . . . . .	69
5	Maximum Deceleration Versus Buoyant Volume Diameter for Varying Lift-Drag Ratios for Mars Equilibrium-Gliding Entry At Subcircular Speeds . . . . .	75
6	Maximum Deceleration Versus Buoyant Volume Diameter for Varying Lift-Drag Ratios for Venus Equilibrium-Gliding Entry at Subcircular Speeds . . . . .	76
7	Maximum Radiation-Equilibrium Surface Temperature (R) Occurring During Planetary Entry for a Sphere . . . . .	81
8	Expandable Heat Shield Deployed and Rigidized Before Entry to Protect a Buoyant Planetary Entry Vehicle . . . . .	84
9	"Airmatt" (Douglas Aircraft Co.) and Rigid Plastic Foam Concepts . . . . .	88
10	Douglas Aircraft Company Concept for Booster Recovery Drag Cone . . . . .	89
11	"Airmatt" Drag Cone Protected Buoyant Planetary Entry Capsule . . . . .	90

<u>Figure</u>		<u>Page</u>
12	A Tension Shell . . . . .	92
13	Buoyant Planetary Probe With Tension Shell Heat Shield Being Constructed in Earth Orbit . . . . .	93
14	Possible Buoyant Planetary Entry Vehicle Configurations . . . . .	97

Notation

<u>Symbol</u>			<u>Units</u>
$A_s$	-	surface area	$\text{ft}^2$
$B_F$	-	buoyant force	lbf
$B_v$	-	buoyant volume	$\text{ft}^3$
$C_D$	-	drag coefficient, dimensionless	
$C_H$	-	total overall heat- transfer coefficient	
$C_L$	-	lift coefficient, dimensionless	
$D$	-	drag force	lbf.
$F_T$	-	sum of external forces on entry vehicle	lbf.
$G$	-	magnitude of deceleration vector felt by an accel- erometer on the entry vehicle	g
$H$	-	heat input to entry vehicle	btu
$L$	-	lift force	lbf
$M$	-	Mach number	
$N$	-	the quantity $\frac{2g_0 W_D}{\beta \sin \gamma_E}$ , dimensionless	
$P$	-	the parameter $\frac{R_e}{M_d}$	ft.
$R$	-	radiation-equilibrium temperature	
$R_e$	-	Reynold's number, dimensionless	
$R_g$	-	range of entering vehicle	ft.
$R_p$	-	radius of planet	ft.
$S$	-	projected surface area	$\text{ft}^2$
$T$	-	temperatures	R

<u>Symbol</u>			<u>Units</u>
$V$	-	velocity of entering body	ft/sec
$W$	-	weight	lbf
$W_D$	-	drag-weight parameter	sec <sup>2</sup> /ft <sup>2</sup>
$W_V$	-	volume-weight parameter, dimensionless	
* * * * *			
$d$	-	diameter of buoyant cell	ft.
$e$	-	base of natural logarithms	
$g$	-	local acceleration of gravity	ft/sec <sup>2</sup>
$h$	-	local height above the surface of the planet	ft.
$\hat{i}, \hat{j}, \hat{k}$	-	unit vectors in $x, y, z$ directions, respectively	
$m$	-	total mass of entering vehicle, slugs	
$m_a$	-	apparent mass of ambient air affected by the buoyant capsule, slugs	
$m_g$	-	mass of gas inside the buoyant cell, slugs	
$m_s$	-	structural mass of entry vehicle, slugs	
$r$	-	distance from origin of inertial coordinate system to the center of gravity of the entering vehicle	ft.
$t$	-	time	sec.
$y$	-	local density ratio, equal to $\rho/\rho_0$ , dimensionless	

SymbolUnits

\* \* \* \* \*

$\beta$	-	atmospheric scale-height constant of a planetary atmosphere	ft. <sup>-1</sup>
$\gamma$	-	angle between the local horizon and the velocity vector, positive as drawn on figures 1 and 4, degrees or radians	
$\epsilon$	-	surface emissivity of entry vehicle	
$\theta$	-	angle between a reference line and the position vector $\vec{r}$ , degrees or radians	
$\rho$	-	local atmospheric density, slugs per cubic ft.	
$\sigma_B$	-	Boltzmann's constant	
$\phi$	-	the angle $\gamma + \theta$	
$\omega$	-	angular velocity of the rotating body axes of the entry vehicle with respect to inertial coordinates	
		radians / sec.	

Subscripts

E	-	conditions at entry
F	-	force
m	-	conditions at maximum deceleration



Subscripts (Continued)

$MAX$	-	maximum
$0$	-	value at the surface of the planet
$r$	-	in direction of $r$
$y$	-	in direction of $y$
$z$	-	in direction of $z$

Mathematical Notation

$(\hat{\phantom{a}})$	-	denotes a unit vector
$(\dot{\phantom{a}})$	-	first derivative of the quantity ( ) with respect to time
$(\ddot{\phantom{a}})$	-	second derivative of the quantity ( ) with respect to time
$(\vec{\phantom{a}})$	-	vector quantity
$\ln( )$	-	natural logarithm of ( )
$\equiv$	-	"is identically equal to"
$<$	-	"less than"
$>$	-	"greater than"
$\ll$	-	"much less than"
$\exp( )$	-	the base of natural logarithms raised to the power ( )
$(\vec{\phantom{a}}) \times (\vec{\phantom{a}})$	-	cross product of two vector quantities
$\rightarrow$	-	"approaches"
$\frac{d(A)}{d(B)}$	-	derivative of (A) with respect to (B)
$d(A)$	-	differential of (A)
$\int$	-	integral

Abstract

Providing an entry vehicle with a large buoyant volume permits a useful alternative method of unmanned planetary exploration. This type of vehicle could be used to float an instrument package in a planetary atmosphere for a considerable time, or to "soft land" a payload on the surface of a planet without using parachutes or retrorockets.

In this study, it was assumed that the large buoyant volume is deployed prior to atmospheric entry. The effect of buoyancy on the entry dynamics was investigated, using a first-order entry model. That is, a two-dimensional entry trajectory, a perfectly spherical planet, a constant gravity, and no wind were assumed. It was found that the effect of buoyancy on the velocity, maximum deceleration, and altitude of maximum deceleration of planetary entry vehicles is insignificant. This is true for all entry angles, even if the entry velocity is decreased considerably by rocket braking, and even if the buoyant volume diameter is very large (greater than 500 feet). There is one case, however, for which the buoyant effect is not altogether insignificant, though still small. This is the case of equilibrium-gliding entry. For example, for constant lift-drag ratios of 0.1 and spherical buoyant volume diameters of 300 feet, the maximum deceleration is decreased by 2.6% for Mars and 1.8% for Venus from the value of maximum deceleration for non-buoyant entry vehicles. For constant lift-drag ratios of 1.0 and diameters of 300 feet, the maximum deceleration is decreased by 0.8% for Mars and 0.7% for Venus.

For buoyant planetary entry, the heating problem can be solved by several methods. These methods fall into two classes: the use of expandable heat resistant structures permitting direct launch from the surface of the Earth, and constructing a heat-resistant shield around the buoyant volume and launching while in Earth orbit. The first of these methods would entail using expandable heat-resistant materials which could be expanded to protect the buoyant envelope prior to entry. To further decrease the entry heat load, the vehicle could be maneuvered into a circular orbit around the planet. A natural orbit-decay entry or equilibrium-gliding entry would then follow. The drag cone concept using expandable "airmatt" materials for heat protection appears most promising. In the second method, a cone or tension shell structure would be constructed around the buoyant volume while in Earth orbit. This would permit direct planetary entry at hyperbolic speeds and would involve minimum guidance and no deploying of expandable structures. In both of the above methods, the heat shield would be discarded after entry is complete.

In summary, it is believed that scientific payloads could be delivered to the surface of planets in "soft" landings, without using retrorockets, by means of the capsule's buoyancy within the atmosphere. The payloads would be modest for Mars, but considerable for Venus. Buoyant payloads could also be floated in the atmospheres of Venus, Mars, and other planets, providing a unique means of collecting a great deal of data.

	<u>Contents</u>	<u>Page</u>
Preface . . . . .		ii
List of Figures . . . . .		iii
Notation . . . . .		v
Abstract . . . . .		ix
I. Introduction . . . . .		1
Background . . . . .		1
Methods of Unmanned Planetary Exploration. . . . .		3
Unmanned Planetary Exploration by Buoyant Capsules . . . . .		4
Types of Balloons . . . . .		7
Limitations . . . . .		7
Statement of the Problem . . . . .		8
Scope of the Study . . . . .		8
Limits of the Study . . . . .		9
Analysis of the Problem . . . . .		9
Assumptions . . . . .		12
Summary of Current Knowledge About the Problem. . . . .		14
Organization of Remainder of the Thesis . . . . .		15
II. Entry and Terminal Dynamics . . . . .		16
Entry Dynamics . . . . .		16
Assumptions . . . . .		16
Analysis . . . . .		18
Lift and Drag Force Representation . . . . .		27
Buoyant Force Representation . . . . .		30
Analytical Solutions . . . . .		34
Entry at Large Angles With Zero Lift . . . . .		34

	<u>Contents Cont'd</u>	<u>Page</u>
	Vertical Entry With Zero Lift . . . . .	40
	Variable Lift-Drag Ratio Entry (Constant Flight-Path Angle) . . . . .	42
	Gliding Entry From Circular Satellite Orbit at Small Flight- Path Angles With Constant Lift- Drag Ratio . . . . .	44
	Gliding Entry at Supercircular Speeds at Small Entry Angles With Constant Lift-Drag Ratio . . . . .	52
	Equilibrium Gliding Entry at Small Flight-Path Angles with Constant Lift-Drag Ratio . . . . .	58
	Terminal Dynamics . . . . .	66
	Discussion of Results . . . . .	73
III.	Gasdynamic Heating . . . . .	77
	General . . . . .	77
	Entry Heating . . . . .	77
	Effect of Buoyancy . . . . .	78
	Entry by Orbital Decay . . . . .	79
	Other Methods of Heat Alleviation . . . . .	82
IV.	Materials, Techniques, and Configurations . . . . .	85
	Materials . . . . .	85
	Tension Shell Structure . . . . .	91
	Spinning Spherical Entry Bodies . . . . .	94
	Optimum Compromise Between Minimum Retro-Rocket Braking and Buoyant Force Contribution . . . . .	94
	Configurations . . . . .	96
V.	Conclusion and Recommendations . . . . .	98
	Conclusions . . . . .	98

Contents Cont'd

	<u>Page</u>
Recommendations for Further Study . . . . .	100
Bibliography . . . . .	101
Appendix A: Characteristics of Venus and Mars . . . . .	107
Appendix B: Assumption of Negligible Terms . . . . .	108
Vita . . . . .	110

**BLANK PAGE**

## BUOYANT PLANETARY ENTRY

### I. Introduction

This chapter contains a background discussion and statement of the problem. The problem is analyzed and the general assumptions used are listed and discussed.

#### Background

Manned planetary exploration, with Mars and Venus as primary targets, is a firm long-range program (refs 1:69; 2:54;3:1). To support this objective, several unmanned planetary exploration programs are currently underway or in the early planning stages (refs 1:46,102-103;3:1). Many major technical advances will be required before manned planetary exploration will be possible. Of prime necessity is an accurate knowledge of the planetary environment, temperatures, topography, meteorology and, particularly, the atmospheric density, composition, and pressure profiles (refs 1:102-103;3:1,4;sect III, table 3-1). The values and characteristics of these quantities are not accurately known at present.

Besides manned exploration, there is a firm national program for sending unmanned probes to explore the planets for purposes not directly in support of manned visits (refs 14:i,1;15:i,3-4). Chief among these purposes is the search



for extraterrestrial life and the determination of the effect of the planetary environment on terrestrial biology (ref 1:69,102). Dr. R. Festa of the Marshall Space Flight Center has pointed out that instruments are easier to land than men on planets and that machines are adaptable to remote operation in a hostile environment (ref 12:67). Recently, scientists from the Space Sciences Board of the National Academy of Sciences have urged that unmanned probes be sent to Venus to determine if life exists there. They have stated that this is necessary since Mariner II data seem at least questionable (ref 5). (Mariner II was an unmanned probe sent to within 25,000 miles of Venus in 1962 and reported 800 degree F. surface temperature on that planet). The same panel also recommends that Mars be given first priority (after the Apollo programs) for unmanned probes, then the Moon and Venus, Jupiter, Saturn, and the comets and asteroids, in that order.

The exploration of Mars is the focus of scientific interest. Influential scientists both in and out of government have urged an immediate start on flight hardware and experiments for Martian probes "as a scientific undertaking of the greatest validity and significance" (refs 1:69, 102-103;6:69;7:77-83). The exploration of Venus has often been recommended as the next highest priority program.

There are several concepts for unmanned planetary ex-

ploration. This is discussed in the next section.

Methods of Unmanned Planetary Exploration. Most present concepts of unmanned planetary exploration can be placed into one or more of the following classes:

1. The planetary flyby, during which the probe takes pictures and measurements from relatively great distances. Good examples are the Mariner II probe to Venus in 1962 and Mariner 4 to Mars in 1965.

2. The planetary orbiter, in which data are received from a probe placed in orbit around the planet. The Lunar Orbiter program is an example.

3. Direct collision, such as the Ranger lunar probes in which data are transmitted before the capsule is destroyed by impact. Such capsules may be launched directly from earth or from another vehicle in a flyby or orbiter trajectory.

4. Landing a capsule gently on the surface by means of retrorockets or parachutes. The Surveyor and Voyager programs are examples.

All of these methods have advantages and disadvantages for particular missions. In this study it is proposed that another method of unmanned planetary exploration be investigated: an instrumented capsule suspended in the atmosphere of a planet by means of a balloon or similar buoyant structure. Some ideas to support the thesis that it would be scientifically useful to do this are presented below.

Unmanned Planetary Exploration by Buoyant Capsules.

A capsule that could be suspended in the atmospheres of planets like Venus, Mars, Jupiter, and Saturn could provide a great deal of useful information. In fact, such a capsule could provide as much information as several unmanned vehicles using the other methods. For example, a "flyby" or orbiting vehicle could not determine the existence of life; a collision vehicle's lifetime and amount of data that it could transmit are limited; even a landed vehicle is limited by its environment, unless it were mobile, and even then it is limited by terrain and fuel. In the case of Mars, the extremely thin atmosphere (as reported by Mariner 4) of 5-8 millibars at the surface will probably necessitate retro-rockets for a gentle landing, or parachutes for a "hard" but survivable surface landing (ref 8:66-69). If retro-rockets are used, several serious difficulties are foreseen. Using retro-rockets close to the ground could seriously disrupt the data gathering; the heat could alter the biological character of the Martian surface. If the retro-rockets were used higher to avoid this, impact speeds would increase, possibly damaging or destroying the instruments. (ref 9:55)

In contrast to the above, a vehicle suspended in the atmosphere could take closeup pictures of large areas of the planet, unlimited by terrain or fuel. It could take direct measurements and make direct analyses of atmospheric temperatures, densities, and compositions at many

different locations on the planet. It could repeat these analyses for comparison and greater statistical reliability. It could provide the means for a very accurate determination of winds at various altitudes; and it could give scientists on earth a real-time closeup view, as all this is being done, of large areas of the planet from different perspectives.

As previously mentioned, the search for extra-terrestrial life is probably the most basic goal in unmanned planetary exploration. (refs 7:70;37:1) The question of whether there is extraterrestrial life may well solve the question of the biological origin and evolution of life (ref 10:1). The Earth's atmosphere contains billions of living microscopic organisms. Bacteria, algae, fungi, and other micro-organisms are commonly found. In addition to this, fossil forms and fragments and parts of organisms such as seeds, pollen, and spores are also frequently found in the atmosphere (ref 10:13). It may well be expected that some of these components would be found in the atmosphere of a planet if life exists there. It therefore is unnecessary that a capsule actually be landed on the surface to determine if life exists. Atmospheric samples could be collected over large areas by the suspended capsules, and a variety of biochemical tests could be performed with greater reliability and statistical meaning. Indeed, some scientists have speculated that life on Venus may be suspended within the atmosphere, or located

on the peaks of high mountains (ref 11).

It is also within the realm of possibility that the capsule could be landed on the planet, then flown again to come down at another point, an advantage not obtainable with other means of exploration. Dr. Morris Topper, director of NASA'S meterological programs, has urged that a Martian weather forecasting system be established to preceed manned missions to that planet. The system would use a Martian polar orbiting satellite and a series of balloons floating in the Martian atmosphere (ref 12:67). The satellite would interrogate the balloons for weather data and transmit the information to a central station or approaching spacecraft. This is of some interest since high winds are thought to move around the planet.

There are some differences between balloon flight on the earth and on the other planets. Of course, there are many similarities, too. There have been many recent advances in balloon technology for scientific research, and continuing research will provide further improvements. Presently, research balloons can carry relatively large, heavy scientific payloads to altitudes where the pressure is only 2 millibars (ref 13:42). Since the Martian atmosphere is estimated at 5-8 millibars, it is possible that some type of balloon could suspend a scientific payload even in that thin atmosphere.

Balloons are very stable and experience few disturbing forces, since they move with the wind as part of it.

Research balloons rotate no more than one revolution per hour and oscillate negligibly. One experiment has been able to track celestial targets to accuracies of  $1/3$  of an arc-second for up to 2 hours, with  $1/60$  arc-second tracking appearing feasible (ref 13:46-47).

Types of Balloons. There are two basic types of balloons that are of interest in this study. There are the "zero-pressure" vented balloon and the superpressure balloon. Zero-pressure balloons can carry 12,000 lbs. to earth altitudes of 80,000-100,000 ft. (about 28-11 mb) with reliabilities above 80%. Loads up to 500 lb. can be carried to 130,000 ft. (about 3 mb) at reliabilities of approximately 75%. Loads of up to 200 lb. will reach 140,000-145,000 ft. (about 2-1.8 mb) with about 75% reliability (ref 13:47). The zero-pressure balloon capsule must drop 5-7% of its gross weight as ballast at each sunset if it is desired to maintain altitude. This limits the useful life to about a week.

The superpressure balloon is a closed, unvented vessel made of strong materials so that the volume remains constant. The balloon will then float at a constant density altitude and needs to drop no ballast at sunset. Superpressure balloons can easily carry loads of 40 lbs. and several flights have been made with nearly 300 lbs. (ref 12:47).

Limitations. Although the vertical rates of descent and

ascent of a balloon are controllable, it cannot be steered or guided. It must go where the wind goes. Further, the skin must be very light.

With the above considerations in mind, the problem to be investigated in this study will be defined in the next section.

### Statement of the Problem

The problem is to derive the laws governing the dynamics of buoyant atmospheric entry, to interpret the effect of buoyancy on the entry dynamics and thermodynamics, and to derive the laws governing the subsequent free motion of the buoyant capsule in the planetary atmosphere.

Scope of the Study. In general, this will be a first order study. That is, the perturbative effects due to the oblateness of a planet and an unsymmetrical, rotating atmosphere will be neglected. Analytic solutions will be obtained by making justifiable assumptions to linearize the equations of motion. These subjects will be treated:

1. The general equations of motion for the buoyant vehicle during and after entry.
2. Interpretation of the effects of buoyancy on the dynamics and thermodynamics of non-buoyant entry previously studied by others.
3. A discussion of heating effects, materials, configurations, and techniques.

The results will be presented for the planets Venus and

Mars.

Limits of the Study. This study will not include the structural design of the spacecraft beyond general shape considerations. Nor will it contain a detailed treatment of the guidance, control, and communications systems beyond general considerations. The study will be restricted to analytic solutions.

Analysis of the Problem

A vehicle approaching a planetary atmosphere possesses a large amount of energy; kinetic energy due to its motion and potential energy due to its altitude above the surface. The kinetic energy is much the greater when the vehicle is still outside the atmosphere. As the vehicle begins to enter the atmosphere, the drag due to the friction of the atmospheric gases begins to slow it down. The kinetic energy of the vehicle is dissipated in the form of heat. A large part of this heat can be diverted away from the vehicle skin. However, a significant portion of the heat is transferred to the vehicle, causing high skin and internal temperatures. This is the first critical problem of planetary entry. The second problem is the deceleration experienced by the vehicle. It can be intuitively realized that the higher the angle of penetration into the atmosphere, the higher the deceleration will be. In manned entry, the deceleration problem will be more acute than the



heating problem since the "g's" experienced by the crew must be held to tolerable human levels. For an unmanned vehicle, however, it is clear that relatively high deceleration can be tolerated and that heating is the main problem.

Deceleration and heating are most severe when there is a combination of high atmospheric density and high vehicle velocity; that is, when high velocities are allowed to persist to low altitudes (refs 15:3;17:1,18:9-11,20:2). This situation will exist if the vehicle has initially a high velocity and enters the atmosphere at a large angle. To reduce the heating, therefore, it would seem more practical to enter the atmosphere at as low a velocity and angle as possible. This would tend to restrict the higher velocities to higher altitudes. The initial entry velocity is determined by the planet's gravity and by the type of entry; i.e., directly from space or from an orbit around the planet.

A second factor tending to keep the maximum deceleration and heating at high altitudes, where they are less, is the ratio of drag-surface area to weight of the vehicle. The higher the ratio is, the higher the altitude at which maximum deceleration (and therefore maximum heating) occurs.

A third factor which causes the deceleration and heating to occur at high altitudes is lift. A lifting entry body reduces the rate of descent thus decreasing the maximum deceleration and heating (ref 16:5). Now, if an entering body had a light, buoyant cell there would be

an increase in the lift, drag, and surface area to weight ratio, thus all of the above factors would be enhanced. It is intuitively clear that buoyancy should increase deceleration and decrease heating to the vehicle. Loh (ref 16:6) presents a chart in which thin and fragile materials, (which increase the ratio of area-drag to weight so that deceleration occurs in thinner air and heating is reduced) are shown to reduce maximum nose temperatures from 3200-3600F to 1400-2000F. Significantly, much progress has been made in developing expandable structures made of lightweight materials which are capable of withstanding temperatures up to 1500F and operating at 200,000 ft. (refs 21:41-53;22:74-94;23:501-510). Research has been initiated on expandable structures and fabrics able to withstand speeds greater than Mach 10 and temperatures of 2000F with minimum helium permeability (ref 22:93). All of these factors seem to indicate that a buoyant entry is feasible and eminently possible.

As the entering body is decelerated and heated, the gas inside the buoyant cell could act as a heat sink. If the cell were of the "zero-pressure" vented type, the gas would have a lower density due to the higher temperature and thus enhance the vehicle's initial load carrying ability. If the cell were of the superpressure type, the structural design would have to be stronger to resist the greater internal pressure generated by the heating. After the vehicle has passed its maximum deceleration and

heating points, the velocity, deceleration and heating begin to decrease until the body is in an essentially terminal velocity vertical fall. The weight, buoyant force, and drag will determine the subsequent motion dynamics and the altitude at which the capsule will float.

It is clear what the qualitative effect of buoyancy will be. The remaining problem is quantitative: to what degree will buoyancy effect the entry for various initial conditions of velocity, entry angle, type of entry and vehicle size, weight, drag, and lift parameters? How large a buoyant cell is required? How can the entry heating problem be solved? This study will investigate these and the following further questions: Can buoyancy be used to make a "soft" landing on Mars without using heavy retrorockets? What are the payload capabilities? What are the equations of motion of the terminal dynamics and of the vehicle while floating in the atmosphere? What are the particular configurations, materials, and techniques required to optimize the vehicle and mission?

The general, basic assumptions used in solving the problem are discussed in the next section.

### Assumptions

The following general assumptions are made:

1. The planet is spherically symmetric. This is a good assumption for first order studies, and it is particularly reasonable for the Earth, Venus, and Mars, since these planets have

small equatorial bulges. However, this assumption would be a poor one for Jupiter and Saturn, which have large bulges (ref 24:6).

2. The atmosphere of the planet is spherically symmetric with no winds and is non-rotating. These are reasonable assumptions for an approximate analysis and are commonly made (refs 16-20;24-26).

3. A non-rotating, planetocentric, inertial coordinate system which is assumed to be moving at a constant velocity in a straight line is used. These are good assumptions because: a) the peripheral velocity of the planet is negligible compared to the velocity of the entering vehicle (refs 20:184;24:7-8); and b) the time of entry is measured in minutes during which time the planet has travelled a very small distance in its orbit compared to the total circumference of its path around the sun.

4. The acceleration of gravity is assumed constant and equal to the value on the surface of the planet. This is a reasonable approximation because entry occurs in a very thin shell around the planet so that  $h$  is much less than  $R$  (see list of nomenclature). On Earth, for example, the acceleration of gravity decreases by only 1% for every 100,000 feet increase in altitude.

5. The entry vehicle experiences no side forces and has zero angle of bank with "wings level" throughout the entry trajectory. This assumption is necessary to

restrict the problem to two dimensions. This assumption is commonly used (refs 16-19; 20:99-101;24-27).

The effect of these assumptions is to restrict the entry trajectory to a plane which describes a great circle on the surface of the planet. This reduces the problem to one of two dimensions. No significant limitations on the validity of the results will be introduced by these assumptions. The salient features of the motion and behavior of the type of vehicle being considered will be adequately revealed to a good first approximation (refs 16-20, 24-27).

There are other assumptions and approximations of a mathematical, rather than physical, nature. These will be introduced at the appropriate points in the analyses.

#### Summary of Current Knowledge About the Problem.

The general dynamics and thermodynamics principles of planetary entry have been well known for many years. In fact, serious scientific studies on interplanetary missions and planetary entry go back to the 1920's with the work of Hohmann and others (ref 4, ppl-1) and to the early 1930's with the work of Sänger (refs 24:2;28:1141). The amount of material published on the general subject of planetary entry since the early and middle 1950's has been vast. Nearly every facet of the subject has been studied extensively. Two brief mentions have been found by the writer on the subject of floating balloons in the atmospheres of planets (refs 12:67 and 15:4).

Continuing progress has been made on the subject of lightweight but strong inflatable structures which can survive the heat of entry (refs 21:40-53; 22:74-94, 23:501-510; 29:101, 30:95-117). But no application has been made, far as the writer has been able to determine, of these principles to the analysis of the effects of buoyancy on entry dynamics and thermodynamics and to the concepts of buoyant planetary exploration capsules.

#### Organization of Remainder of the Thesis

The following chapter contains the development of the entry and terminal dynamics and the analytical solutions for a buoyant planetary entry vehicle. Chapter III contains a discussion of the heating effect and Chapter IV contains a discussion of materials, configurations, and techniques. Conclusions and recommendations are given in the final chapter. Appendix I contains a short list of the atmospheric and gravitational characteristics of Venus and Mars as used in this study (these data were taken from references 8 and 19). Figures and graphs are contained within the text.

## II. Entry and Terminal Dynamics

This chapter contains the development of the general equations of motion of buoyant planetary entry and of a buoyant capsule floating in a planetary atmosphere. Linearizing assumptions are made which permit analytic solutions of the equations for certain regimes of entry. The analytic solutions are then applied to the buoyant entry of Venus and Mars.

### Entry Dynamics

The two-dimensional coordinate frame used in developing the entry dynamics is shown in figure 1. The  $x$  body axis always points in the direction of the velocity vector of the entering vehicle. The  $z$  body axis is perpendicular to the  $x$  axis and is in the plane described by the velocity vector and the attracting center of the planet. The  $y$  body axis is perpendicular to the  $x-z$  plane.

Assumptions. The following assumptions are made:

1. The lift (if any) and drag of the entering vehicle act in a direction perpendicular and opposite, respectively, to the velocity vector.
2. The vehicle consists of a buoyant cell and one or more instrument capsules. The total volume of the instrument capsules is assumed to be much less than the volume of the buoyant cell.

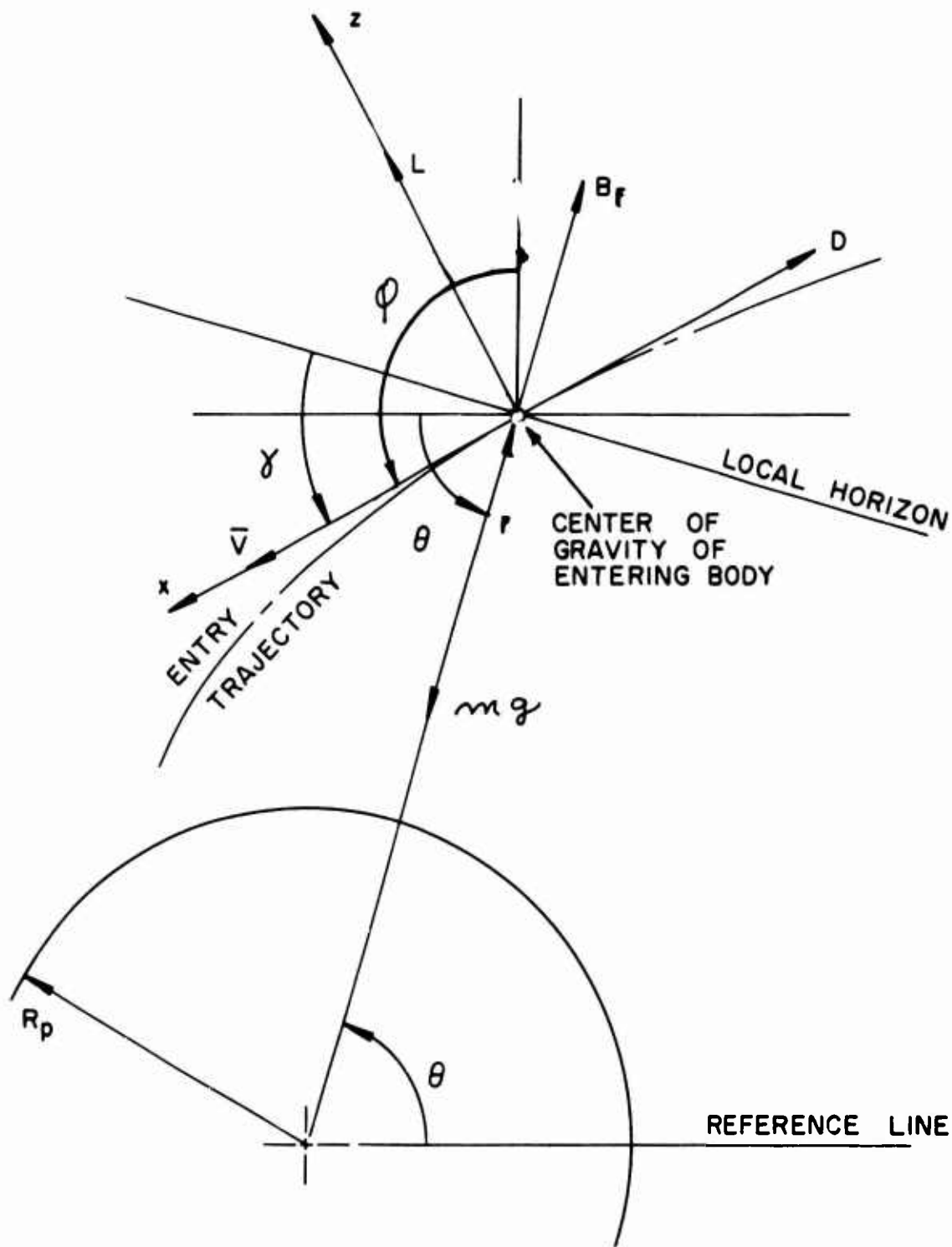


Fig. 1

Coordinate System for Buoyant  
Planetary Entry



3. The mass of the vehicle is divided into two parts, the structural mass (including the skin of the buoyant cell), and the mass of gas within the buoyant cell.

Analysis. The gravity force acts directly toward the attracting center of the planet. The buoyant force acts in a direction opposite to the gravity force and through the center of gravity of the displaced fluid (refs 31:59-60;32:37-39).

Figure 2 shows a generalized entry configuration.  $M_L$ ,  $M_D$ , and  $M_B$  are the moments about the center of gravity of the vehicle due to the lift, drag, and buoyant forces, respectively. These moments are caused by the fact that the point of application of the lift, drag, and buoyant forces does not in general coincide with the center of gravity of the vehicle. In this study the effects of these moments on stability and the resulting oscillations of the entry vehicle are not considered. It must be kept in mind, however, that these moments may be negative or positive in the general case, and that they may be cancelled out by the auxilliary aerodynamic surfaces. For spheres and some other symmetric configurations, the moments due to the drag and buoyant forces are, of course, zero.

In figure 1, the unit vectors for the body axes  $(x,y,z)$  are  $(\hat{x}, \hat{y}, \hat{z})$ , respectively. The position vector to the center of gravity of the body is given by:

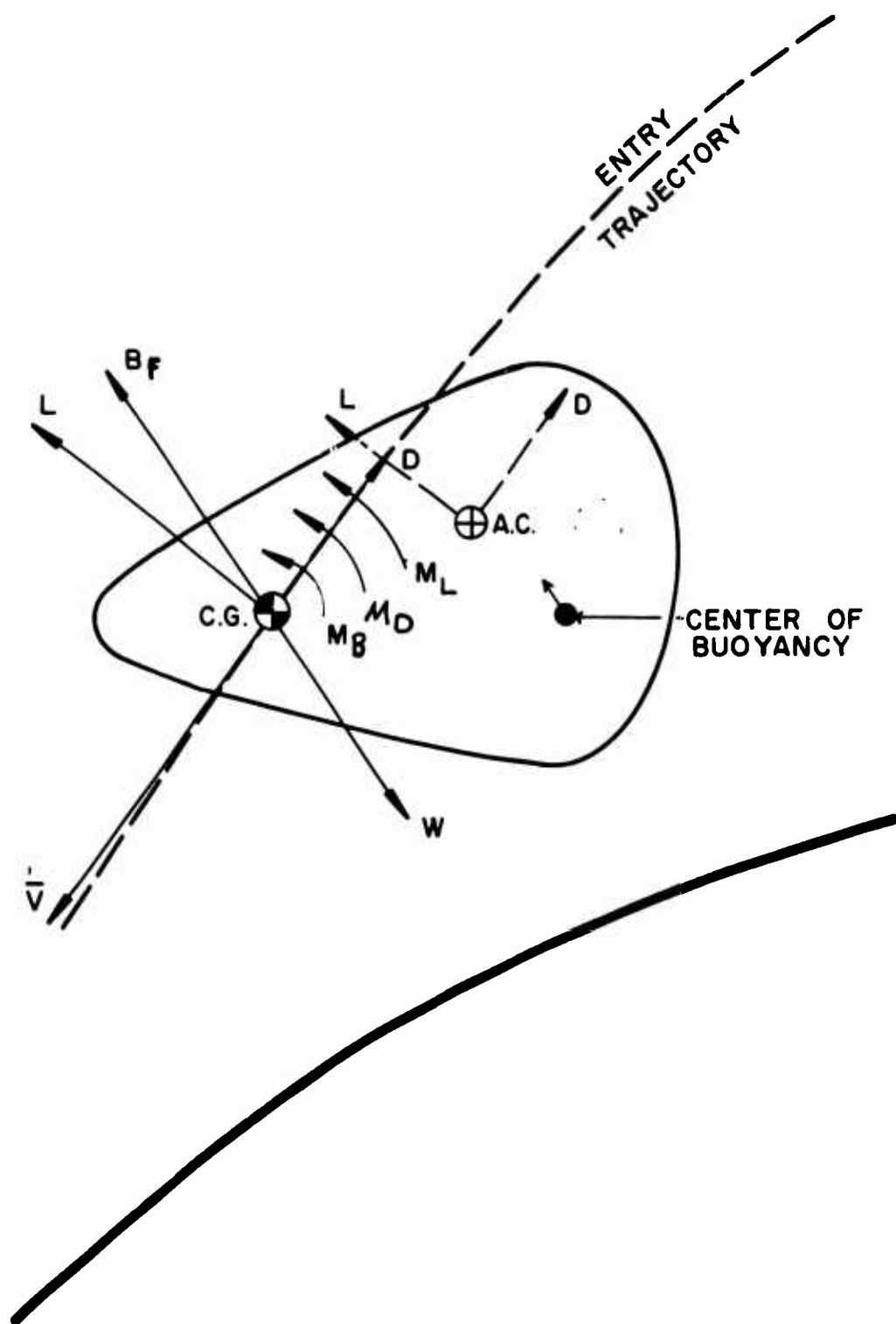


Fig. 2

Moments About the Center of Gravity of an Entry Vehicle Due to the Applied Forces

$$\bar{r} = -r \sin \delta \hat{i} + r \cos \delta \hat{k} \quad (1)$$

The total force on the body is:

$$\begin{aligned} \bar{F}_T = & (-D - B_F \sin \delta + mg \sin \delta) \hat{i} + \\ & (L + B_F \cos \delta - mg \cos \delta) \hat{k} \end{aligned} \quad (2)$$

The total force is also defined by:

$$\bar{F}_T = F_x \hat{i} + F_z \hat{k} \quad (3)$$

where  $F_x$  and  $F_z$  are the  $\hat{i}$  and  $\hat{j}$  components as given in eq (2). Eq (1) is differentiated with respect to time to obtain:

$$\begin{aligned} \dot{\bar{r}} = & -(r \cos \delta \dot{\delta} + \dot{r} \sin \delta) \hat{i} + \\ & (-r \sin \delta \dot{\delta} + \dot{r} \cos \delta) \hat{k} + \\ & \bar{\omega} \times \bar{r} \end{aligned} \quad (4)$$

where  $\bar{\omega}$  is defined as the angular rotational velocity of the body axes (x,y,z) with respect to the planetocentric inertial axes, and is given by

$$\bar{\omega} = \omega_x \hat{i} + \omega_y \hat{j} + \omega_z \hat{k} \quad (5)$$

Performing the vector multiplication indicated in eq (4) by using eqs (1) and (5),

$$\begin{aligned}\bar{\omega} \times \bar{r} = & (r \omega_y \cos \delta) \hat{i} + \\ & (-r \omega_z \sin \delta - r \omega_x \cos \delta) \hat{j} + \\ & (r \omega_y \sin \delta) \hat{k}\end{aligned}\quad (6)$$

Substituting eq (6) into eq (4),

$$\begin{aligned}\dot{\bar{r}} = & (-r \cos \delta \dot{\delta} - \dot{r} \sin \delta + r \omega_y \cos \delta) \hat{i} + \\ & (-r \omega_z \sin \delta - r \omega_x \cos \delta) \hat{j} + \\ & (-r \sin \delta \dot{\delta} + \dot{r} \cos \delta + r \omega_y \sin \delta) \hat{k}\end{aligned}\quad (7)$$

$\dot{\bar{r}}$  may also be defined as follows:

$$\dot{\bar{r}} \equiv \bar{v} = v_x \hat{i} + v_y \hat{j} + v_z \hat{k}\quad (8)$$

Comparing eqs (7) and (8),

$$v_x = -r \cos \delta \dot{\delta} - \dot{r} \sin \delta + r \omega_y \cos \delta\quad (9)$$

$$V_y = -r\omega_z \sin \delta - r\omega_x \cos \delta \quad (10)$$

$$\dot{V}_z = -r \sin \delta \dot{\delta} + r \cos \delta + r\omega_y \sin \delta \quad (11)$$

Eq (8) is differentiated with respect to time to obtain

$$\ddot{\vec{r}} = \dot{\vec{V}} = \dot{V}_x \hat{i} + \dot{V}_y \hat{j} + \dot{V}_z \hat{k} + \vec{\omega} \times \vec{V} \quad (12)$$

By using eqs (5) and (8), the vector product  $\vec{\omega} \times \vec{V}$  is:

$$\begin{aligned} \vec{\omega} \times \vec{V} &= (\omega_y V_z - \omega_z V_y) \hat{i} + \\ &(\omega_z V_x - \omega_x V_z) \hat{j} + \\ &(\omega_x V_y - \omega_y V_x) \hat{k} \end{aligned} \quad (13)$$

Therefore, eq (12) becomes

$$\begin{aligned} \dot{\vec{V}} &= (\dot{V}_x + \omega_y V_z - \omega_z V_y) \hat{i} + \\ &(\dot{V}_y + \omega_z V_x - \omega_x V_z) \hat{j} + \\ &(\dot{V}_z + \omega_x V_y - \omega_y V_x) \hat{k} \end{aligned} \quad (14)$$

By Newton's Second Law,

$$\frac{\bar{F}_T}{m} = \dot{\bar{V}} = \ddot{\bar{r}} = \frac{F_x}{m} \hat{i} + \frac{F_y}{m} \hat{j} + \frac{F_z}{m} \hat{k} \quad (15)$$

Therefore, equating the components of eqs (14) and (15),

$$\frac{F_x}{m} = \dot{V}_x + \omega_y V_z - \omega_z V_y \quad (16)$$

$$\frac{F_y}{m} = \dot{V}_y + \omega_z V_x - \omega_x V_z \quad (17)$$

$$\frac{F_z}{m} = \dot{V}_z + \omega_x V_y - \omega_y V_x \quad (18)$$

where  $F_x$ ,  $F_y$  and  $F_z$  are also as given in eqs (2) and (3).

Comparing the components of  $\bar{F}_T$  as given by eq (2) with eqs (16), (17), and (18), the following is obtained:

$$\dot{V}_x + \omega_y V_z - \omega_z V_y = -\frac{D}{m} + g \sin \delta - \frac{B_F}{m} \sin \delta \quad (19)$$

$$\dot{V}_y + \omega_z V_x - \omega_x V_z = 0 \quad (20)$$

$$\dot{V}_z + \omega_x V_y - \omega_y V_x = \frac{L}{m} + \frac{B_F \cos \delta}{m} - g \cos \delta \quad (21)$$

Two-dimensional motion has been assumed, and the velocity vector is always pointing in the positive x direction.

Therefore,

$$V_y = \dot{V}_y = V_z = \dot{V}_z = 0 \quad (22)$$

Hence, the following replacements can be made:

$$V_x = V \quad (23)$$

and

$$\dot{V}_x = \dot{V} \quad (24)$$

where  $V$  is the magnitude of the absolute velocity of the entering vehicle with respect to the planetocentric inertial coordinates. Substituting eqs (22), (23), and (24) into eqs (19), (20), and (21),

$$\dot{V} = -\frac{D}{m} - \frac{B_F \sin \delta}{m} + g \sin \delta \quad (25)$$

$$-V\omega_y = +\frac{L}{m} + \frac{B_F \cos \delta}{m} - g \cos \delta \quad (26)$$

$$V \omega_z = 0 \quad (27)$$

From eq (27),

$$\omega_z = 0 \quad (28)$$

Since the vehicle maintains zero bank (assumption 5, page 13),  
and from eqs (10) and (22),

$$\omega_x = 0 \quad (29)$$

From eqs (9), (11), (22), and (23)

$$V = -r \cos \delta \dot{\delta} + r \omega_y \cos \delta - \dot{r} \sin \delta \quad (30)$$

$$0 = -r \sin \delta \dot{\delta} + r \omega_y \sin \delta + \dot{r} \cos \delta \quad (31)$$

The angular position of the vehicle can be measured in polar coordinates by the angle  $\theta$ , given in figure 1. The angle between the positive  $x$  body axis and a fixed reference line is given by the angle  $\phi$ . From figure 1,

$$\phi = \delta + \theta \quad (32)$$



The rate of change of  $\phi$  with respect to time is  $\omega_z$ :

$$\omega_z = \dot{\phi} = \dot{\gamma} + \dot{\theta} \quad (33)$$

Therefore, substituting eq (33) into eqs (30) and (31):

$$V = -r \cos \gamma \dot{\gamma} - \dot{r} \sin \gamma + r \cos \gamma (\dot{\gamma} + \dot{\theta}) \quad (34)$$

$$0 = -r \sin \gamma \dot{\gamma} + \dot{r} \cos \gamma + r \sin \gamma (\dot{\gamma} + \dot{\theta}) \quad (35)$$

Simplifying eqs (34) and (35),

$$V = -\dot{r} \sin \gamma + r \dot{\theta} \cos \gamma \quad (36)$$

$$0 = \dot{r} \cos \gamma + r \dot{\theta} \sin \gamma \quad (37)$$

Multiplying eq (36) by  $\cos \gamma$  and eq (37) by  $\sin \gamma$  and adding the resulting equations yields:

$$r \dot{\theta} = V \cos \gamma \quad (38)$$

Multiplying eq (36) by  $\sin \gamma$  and eq (37) by  $\cos \gamma$  and subtracting the resulting equations, one obtains:

$$\dot{r} = -V \sin \gamma \quad (39)$$

Eqs (38) and (39) together with eqs (25) and (26) are the basic non-linear equations of motion. Substituting eq (33) into eq (26) they may be rewritten as:

$$\dot{V} = -\frac{D}{m} + \frac{mg \sin \gamma}{m} - \frac{B_F \sin \gamma}{m} \quad (40)$$

$$V(\dot{\gamma} + \dot{\theta}) = -\frac{L}{m} + \frac{mg \cos \gamma}{m} - \frac{B_F \cos \gamma}{m} \quad (41)$$

$$r \dot{\theta} = V \cos \gamma \quad (42)$$

$$\dot{r} = -V \sin \gamma \quad (43)$$

Lift and Drag Force Representation. Lift and drag may be related to the velocity and density in terms of the dimensionless parameters  $C_L$  and  $C_D$  by following expressions:

$$L = \frac{C_L S}{2} \rho V^2 \quad (44)$$

$$D = \frac{C_D S}{2} \rho V^2 \quad (45)$$

Where  $\rho$  is the local atmospheric density,  $S$  is the projected reference area of the body, and  $C_L$  and  $C_D$  are dimensionless aerodynamic lift and drag coefficients, respectively. The aerodynamic coefficients  $C_L$  and  $C_D$  are, in general, functions of velocity, angle of attack, and the shape of the vehicle (ref 20:84). At high altitudes (above about 125 miles for Earth) gas flow is in a free molecule regime. If the Mach number is above about 5,  $C_D$  can be taken as a constant (range  $2.1 < C_D < 2.3$ ) for spheres, cones, and cylinders (ref 33:185-186; also see ref 34, pp 15-19), and is approximately invariant with the vehicle's shape and mechanism of molecular interaction with the vehicle's surface (ref 19:3). The lift force, in contrast, depends strongly on the shape of the vehicle and on the molecular interaction with the surface.

It is a commonly made simplifying assumption (refs 16:20; 24:28) that  $C_L$  and  $C_D$  are invariant with velocity and altitude, since entry occurs at high altitudes and at high velocities. It should be kept in mind, however, that both these quantities may be varied by auxiliary aerodynamic lift and drag devices which it may be desirable to use for particular missions. This is called lift and drag "programming" or "modulation". Such means are, however, difficult to achieve in practice and introduce additional weight and complexity into the system (ref 20:186).

A further approximation which is often made is the

assumption of an isothermal atmosphere in hydrostatic equilibrium. This enables the local density to be written as a function of altitude by the barometric equation:

$$\rho = \rho_0 e^{-\beta h} \quad (46)$$

where  $\rho_0$  is the surface value of atmospheric density,  $h$  is local altitude above the surface, and  $\beta$  is the atmospheric scale height for the particular planet, given by (ref 19:7):

$$\beta = -\frac{1}{\rho} \frac{d\rho}{dh} \quad (47)$$

This assumption of an exponentially varying atmosphere is based on the kinetic theory of an isothermal gas in a constant gravity field (see for example, ref 35:18-19).

The planetary atmospheres are not perfectly isothermal. Nevertheless, their atmospheric density distribution can be approximated reasonably well by eq (46) (refs 19:7 and 24:6-7). In any real atmosphere,  $\beta$  varies with altitude. For general entry studies, however,  $\beta$  may be taken as a constant for a particular planet (ref 16:12).

For convenience, a definition is made that

$$y \equiv e^{-\beta h} \quad (48)$$

so that

$$\dot{y} = -\beta \dot{h} y \quad (49)$$

Since

$$h = R - R_p \quad (50)$$

eq (49) may be written as

$$\dot{y} = -\beta \dot{r} y \quad (51)$$

Substituting eqs (46) and (48) into eqs (44) and (45),

$$\frac{L}{m} = \frac{C_L S}{2mg_0} g_0 \rho_0 y V^2 \quad (52)$$

$$\frac{D}{m} = \frac{C_D S}{2mg_0} g_0 \rho_0 y V^2 \quad (53)$$

Buoyant Force Representation. According to Archimedes' principle the buoyant force  $B_F$  is equal to the weight of atmosphere displaced by the buoyant volume. Therefore,

$$B_F = m_{ATM} g \quad (54)$$

since mass equals density times volume, and  $g = g_0$ , by assumption 4, page 13 ,

$$B_F = \rho B_v g_0 \quad (55)$$

where  $B_v$  is buoyant volume of the entering vehicle.

Substituting eq (46) into eq (55),

$$\frac{B_F}{m} = \rho_0 g_0 \frac{B_v}{m} \gamma \quad (56)$$

The following definitions are made for convenience:

$$\frac{C_D S}{m g_0} \frac{\rho_0}{2} \equiv W_D \quad (57)$$

$$\frac{\rho_0 g_0 B_v}{m g_0} \equiv W_v \quad (58)$$

$W_D$  is the "drag-weight" parameter and  $W_v$  is the "volume weight" parameter. Both are constant.

From assumption 4,

$$g \cong g_0 \cong \text{CONSTANT} \quad (59)$$

The variation of gravity with altitude is given by (ref 36:23):

$$g = g_0 \frac{R_p^2}{r^2} \quad (60)$$

Eq (59) therefore implies that

$$r \cong R_p \cong \text{CONSTANT} \quad (61)$$

This is a reasonable assumption since the whole entry takes place in a thin shell around the planet so that  $h$  is much less than  $R_p$ . Further, as entry progresses,  $r \rightarrow R_p$ .

If eqs (52), (53), (56), (57), (58), and (59) are substituted into eqs (40), (41), (42), and (43), there results:

$$\dot{V} = -g_0 W_D y V^2 - g_0 W_V y \sin \delta + g_0 \sin \delta \quad (62)$$

$$V(\delta + \epsilon) = -g_0 \frac{L}{D} W_D y V^2 - g_0 W_V y \cos \delta + g_0 \cos \delta \quad (63)$$

$$\dot{h} = -V \sin \gamma \quad (64)$$

$$h \dot{\theta} = V \cos \gamma \quad (65)$$

These are the basic non-linear differential equations of motion, with four equations in four unknowns.

The preceeding analysis was for the buoyant cell expanded or deployed prior to entry. Several other profiles for the balloon mission are possible. These are: a) landing a capsule gently on the surface by means of retrorockets, then inflating the balloon; b) deploying the buoyant cell during the terminal descent; c) deploying the buoyant cell at some point in the entry trajectory prior to the terminal descent. The first two methods are marginal on the basis of the uncertainty in the wind velocities and vertical wind gradients in the planetary atmospheres. Mars, particularly, is thought to have very high winds both on the surface and in the atmosphere (refs 8:67,69; 38:4-10). Balloons are notoriously difficult to inflate and land in winds greater than 10-15 mph and then only with skilled handlers (ref 13:44). The third method would involve greater risks at no advantage to inflating the cell before entry. In all three of these methods, inflation would have to be carried out against outside air loads, pressures, and heating, which greatly increases the possibility of



failure. It would seem more practical to inflate the cell before entry where the problem is greatly simplified. Methods for rigidization of light inflatable structures in space are under development (refs 39:236-254; 40:369-380). This process is desirable to avoid deformation buckling, and ripping of the buoyant cell due to winds or other planetary environmental hazards. Rigidization would be most easily carried out in space and could also provide means to overcome the entry heating problem.

#### Analytical Solutions

Unfortunately, a general closed form analytical solution for eqs (62)-(65) is not possible, and numerical techniques must be used. However, simplifying assumptions (which hold over limited regimes) can be made which permit certain approximate analytical solutions. Many authors have used this approach to obtain analytic solutions (refs 16-20; 24-28), and this is the procedure which will be followed in this section. The resulting graphs will be presented and discussed in a separate section of this report.

A general assumption that is made is that the buoyant cell is essentially rigid and non-deformable so that the buoyant volume remains constant.

Entry at Large Angles With Zero Lift. Allen and Eggers (ref 27) were the first to use steep entry, constant flight-path angle assumption. The basic assumptions are:

1.  $L = 0$

$$2. \quad m g \sin \gamma \ll D + B_F \sin \gamma$$

This assumption is commonly made. Neglecting vehicle weight does not materially affect the results (ref 27:1127; 17:5). In this entry mode, drag and buoyancy are assumed to dominate the deceleration.

3. The term  $(1 - \frac{V^2}{gR} - W_V \gamma) g \cos \gamma$  is negligible at large angles and at the altitudes where the most significant effects occur.

Incorporating these assumptions into the equations of motion (62) to (65), one has

$$\dot{V} = -g_0 W_D \gamma V^2 - g_0 W_V \gamma \sin \gamma \quad (66)$$

$$\dot{\gamma} = 0 \quad (67)$$

$$\dot{h} = -V \sin \gamma \quad (68)$$

Eq (67) implies that

$$\gamma = \gamma_E \quad (69)$$

$$\gamma = \text{CONSTANT} \quad (69a)$$

Using the chain rule, time may be eliminated from eq (66):

$$\dot{V} = \eta \frac{dV}{d\eta} = -g_0 W_D \eta V^2 - g_0 W_V \eta \sin \delta \quad (70)$$

Substituting eqs (51.), (68) and (69) into eq (70) one obtains

$$\frac{dV^2}{d\eta} + \frac{2g_0 W_D}{\beta \sin \delta_E} V^2 = -\frac{2g_0 W_V}{\beta} \quad (71)$$

Eq (71) is of the form

$$(D + N)V^2 = -\frac{2g_0 W_V}{\beta} \quad (72)$$

where  $D \equiv \frac{dU}{d\eta}$  and  $N \equiv \frac{2g_0 W_D}{\beta \sin \delta_E}$ .

Therefore,

$$N = \text{CONSTANT} \quad (72a)$$

$$N = \frac{C_D S \rho_0}{\beta m} \frac{1}{\sin \delta_E} \quad (72b)$$

The integrating factor is

$$e^{\int N dy} = e^{Ny} \quad (73)$$

The general solution of eq (72) is therefore

$$V^2 e^{Ny} = -\frac{W_V}{W_D} \sin \delta_E (e^{Ny} + \text{CONST}) \quad (74)$$

The boundary (entry) condition is

$$V(y_E) = V_E \quad (75)$$

Therefore, from eq (74)

$$\text{CONST} = -\frac{W_D}{W_V} \frac{V_E^2}{\sin \delta_E} e^{Ny_E} - \frac{e^{Ny_E}}{e^{Ny_E}} \quad (76)$$

and the complete solution of eq (72) is:

$$V^2 = -\frac{W_V}{W_D} \sin \delta_E + \left( V_E^2 + \frac{W_V}{W_D} \sin \delta_E \right) \times e^{-N(y-y_E)} \quad (77)$$

Substituting eq (77) into eq (66), the deceleration is obtained:

$$-\frac{\dot{V}}{g_0} = W_D \left( V_E^2 + \frac{W_V}{W_D} \sin \delta_E \right) \times y e^{-N(y-y_E)} \quad (78)$$

The maximum deceleration is found by putting

$$\frac{d}{dy} \left( -\frac{\dot{V}}{g_0} \right) = 0 \quad (79)$$

Performing the differentiation of eq (78), one finds

$$y_m = \frac{1}{N} = \frac{\beta \sin \delta_E}{2 g_0 W_D} \quad (80)$$

It is interesting to note that this is precisely the same density ratio at maximum deceleration as for non-buoyant steep angle entry (refs 19:13-15; 33:309).

Inserting eq (80) into eq (78), one obtains the maximum deceleration:

$$\left( -\frac{\dot{V}}{g_0} \right)_m = \frac{\beta \sin \delta_E}{2 g_0 e} V_E^2 + \frac{W_V}{W_D} \frac{\beta \sin^2 \delta_E}{2 g_0 e} \quad (81)$$

where  $\mu_E$  is assumed approximately equal to zero. Assuming that the direct approach to the planet is made along a parabolic orbit (ref 17:4) the entry velocity is essentially the escape velocity of the planet. Therefore,

$$V_E^2 = 2 g_0 R_P \quad (82)$$

and eq (81) becomes

$$\left(-\frac{\dot{V}}{g_0}\right)_m = \frac{\beta R_P \sin \gamma_E}{e} + \frac{W_V}{W_D} \frac{\beta \sin^2 \gamma_E}{2 g_0 e} \quad (83)$$

Assuming  $\mu_E \cong 0$  and putting the density ratio at maximum deceleration (eq (80)) into eq (77), the velocity at maximum deceleration may be determined:

$$V_m^2 = \frac{V_E^2}{e} + \frac{W_V}{W_D} \frac{\sin \gamma_E}{e} (1-e) \quad (84)$$

The expressions for velocity, deceleration, maximum deceleration, and velocity at maximum deceleration reduce to the ballistic entry solutions of Gazley, Allen and Eggers, and others (refs 16-19, 26-27) if the volume-

weight parameter is zero. It is interesting to note that the maximum deceleration for buoyant entry depends on the drag, mass, size, and shape characteristics of the vehicle, where in non-buoyant entry the maximum deceleration depends only on the entry angle and the atmospheric and gravitational characteristics of the planet. Eq (84) shows that the velocity at which maximum deceleration occurs is no longer only a function of entry velocity (as in the non-buoyant case), but now depends on the entry angle and the mass, drag, size, and shape of the vehicle as well.

Vertical Entry With Zero Lift. For direct radial entry at parabolic speeds the entry angle remains constant at 90 degrees. The pertinent equations can be written down directly, using the results of the previous section. The density ratio ( $\mu_E$ ) at the entry altitude is assumed to be negligible.

From eq (77), the velocity versus altitude is given by

$$V^2 = -\frac{W_v}{W_D} + \left( V_E^2 + \frac{W_v}{W_D} \right) e^{-N y} \quad (85)$$

From eq (78) the deceleration versus altitude is:

$$\frac{-\dot{V}}{g_0} = W_D \left( V_E^2 + \frac{W_v}{W_D} \right) y e^{-N y} \quad (86)$$

From eq (80), the density ratio at maximum deceleration is:

$$\gamma_m = \frac{\beta}{2g_0 W_D} \quad (87)$$

From eq (81), the maximum deceleration is:

$$\left(-\frac{\dot{V}}{g_0}\right)_m = \frac{\beta V_E^2}{2g_0 e} + \frac{W_v}{W_D} \frac{\beta}{2g_0 e} \quad (88)$$

From eq (84), the velocity at maximum deceleration is:

$$V_m^2 = \frac{V_E^2}{e} + \frac{W_v}{W_D} \left(\frac{1-e}{e}\right) \quad (89)$$

The steep angle entry considered in the previous two sections is the simplest approach to the problem of delivering a payload to a planet. In the following sections, more complex schemes are analyzed. They involve the use of lift, maneuvering the vehicle into a circular orbit around the planet, and other mission profiles



involving guidance accuracies of a very high order. However, as future launch and midcourse correction accuracies are improved, these techniques will become more than merely academic for unmanned vehicles.

Variable Lift-Drag Ratio Entry (Constant Flight-Path Angle) For this entry mode, it is desired to keep the flight-path angle constant. The lift-drag ratio may be programmed to vary as required by aerodynamic means or even by reaction means (ref 16:124). This would enable the vehicle to describe a linear path for all entry angles. The following assumptions are made:

1.  $\frac{L}{D} > 0$
2.  $mg \sin \gamma \ll D + B_F \sin \gamma$
3.  $\gamma = \gamma_E = \text{constant}$

If the flight-path angle is constant, eq (66) can be integrated immediately, after eliminating time as in eq (70). The results of the previous two sections are applicable.

To determine the law under which the lift-drag ratio must be made to vary, eq (63) is used. From assumption 3,  $\dot{\gamma}$  is zero. Therefore eq (63) may be written as:

$$\frac{L}{D} w_D y V^2 = \cos \gamma \left( 1 - w_v y - \frac{V^2}{g r} \right) \quad (90)$$

so that

$$\frac{L}{D} = \frac{\cos \gamma}{W_D \gamma V^2} \left( 1 - W_V \gamma - \frac{V^2}{g R} \right) \quad (91)$$

Eq (77) may be substituted into eq (91) to give:

$$\frac{L}{D} = \frac{\beta \sin 2 \gamma_E}{4 g_0 V^2 W_D^2} \ln \left( \frac{V^2 + a_1}{V_E^2 + a_1} \right) \left\{ \frac{V^2}{g_0 R_P} - \frac{2 g_0 W_V W_D}{\beta \sin \gamma_E} \ln \left( \frac{V^2 + a_1}{V_E^2 + a_1} \right) - 1 \right\} \quad (92)$$

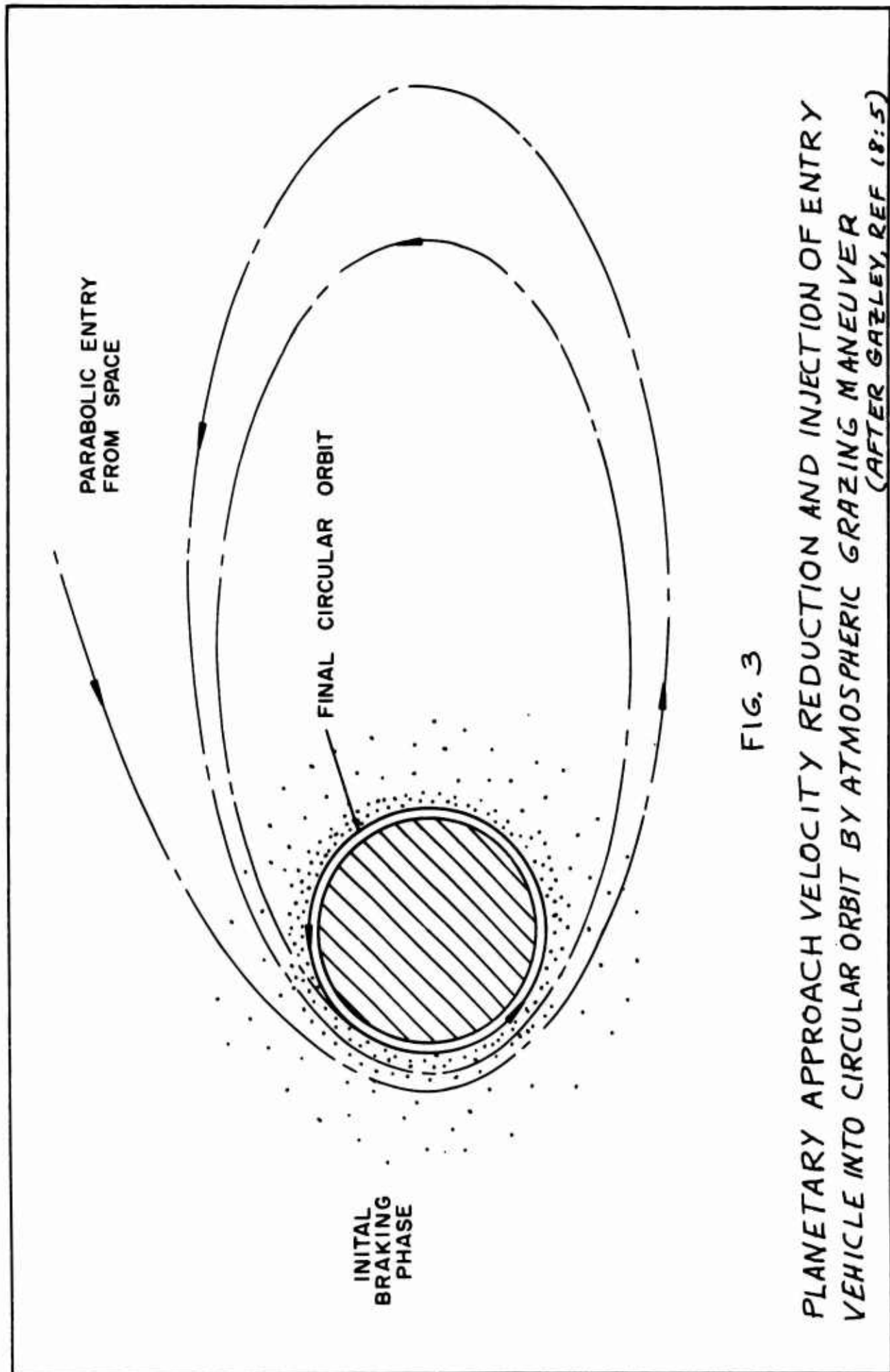
$$a_1 = \frac{W_V}{W_D} \sin \gamma_E \quad (92a)$$

where  $\gamma_E$  is taken to be negligible.

The servomechanism would sense the velocity and vary the lift-drag ratio according to eq (92). There are several possible methods for varying the lift and drag. It has been suggested (ref 41:319-420) that the drag could be modulated by means of flared panels, retractable paddles, or movable spikes which could change the drag coefficient. Another method of drag modulation which has been proposed is the drag brake (ref 42:722-723;36:93). This device is an inverted umbrella-like structure that would be controlled by an accelerometer and a small computer. Lift could be varied by putting aerodynamic

lifting devices on the vehicle and changing the angle of attack of a blunted cone-sphere configuration.

Gliding Entry From Circular Satellite Orbit At Small Flight Path Angles With Constant Lift-Drag Ratio. As stated previously, a combination of high vehicle speed and high atmospheric densities cause the most severe heating problems. It would be profitable, then, to decrease the vehicle speed before entry is initiated without having to pay for it in retro-rocket and propellant weight. One way of doing this would be to maneuver the spacecraft into an orbit around the planet, then enter the atmosphere by allowing the orbit to decay or by initiating a small-angle entry. Although the guidance accuracies required are of a very high order, a vehicle can be maneuvered into an orbit around a planet by performing a grazing maneuver through the planetary atmosphere. This would remove enough energy from the vehicle to lower its velocity below the escape value, if properly performed. The vehicle will then go into an elliptical orbit around the planet (see figure 3), entering the atmosphere at each passage of perifocus (ref 18:3-5). It is known that the vehicle will eventually enter a circular orbit around the planet before it starts to descend through the atmosphere. To speed this process, a drag brake, such as the one described in the previous section, may be deployed at each passage through perifocus. Once the vehicle is in a circular



orbit, it may be allowed to descend through natural decay of the orbit, or entry may be initiated at any angle by thrusting. In the following analysis, it is assumed that entry is initiated at low angles as the analysis of the previous two sections covers the high angle case.

The following assumptions are made:

$$1. \frac{L}{D} > 0$$

2.  $(mg + B_F) \sin \gamma \ll D$  This is a valid assumption for small angles. The vehicle is assumed to be in a regime where the drag force is very large.

3. The term  $(1 - \frac{V^2}{gR}) g \cos \gamma$  is small compared to the lift force and can be neglected. It is to be noted that  $V^2 = gR$  for circular orbits. This equality holds (approximately) during the initial phases of entry (ref 16:73), as the loss in vehicle velocity up to peak deceleration is small when lift is used (ref 26:634).

$$4. \text{ For small } \gamma, \sin \gamma \cong \gamma \text{ and } \cos \gamma \cong 1.$$

With the assumptions, the basic equations of motion, eqs (62) through (65), become

$$\dot{V} = -g_0 W_D \gamma V^2 \quad (93)$$

$$V \dot{\gamma} = -g_0 \frac{L}{D} W_D \gamma V^2 - g_0 W_V \gamma \quad (94)$$

$$\dot{R} = -V \gamma \quad (95)$$

Dividing eq (93) by eq (94), one obtains

$$\frac{1}{V} \frac{dV}{d\gamma} = \frac{1}{\frac{L}{D} + \frac{W_V}{W_D} \frac{1}{V^2}} \quad (96)$$

Manipulating this equation one obtains

$$\int_{\gamma_E}^{\gamma} d\gamma = \int_{V_E}^V \left( \frac{L}{D} \frac{1}{V} + \frac{W_V}{W_D} V^{-3} \right) dV \quad (97)$$

which upon integration yields

$$\gamma - \gamma_E = \frac{L}{D} \ln \left( \frac{V}{V_E} \right) - \frac{1}{2} \frac{W_V}{W_D} \left( \frac{1}{V^2} - \frac{1}{V_E^2} \right) \quad (98)$$

Using eqs (51) and (95) one may write eq (93) as

$$\dot{V} = j \frac{dV}{d\eta} = \beta \gamma \frac{dV}{d\eta} = -g_0 W_D V \quad (99)$$

Substituting eq (98) into eq (99) one obtains

$$\begin{aligned}
 \int_{V_E}^V \left[ \frac{\gamma_E}{V} + \frac{L}{D} \frac{1}{V} \ln \left( \frac{V}{V_E} \right) - \right. \\
 \left. \frac{1}{2} \frac{W_V}{W_D} \frac{1}{V^3} + \right. \\
 \left. \frac{1}{2} \frac{W_V}{W_D} \frac{1}{V_E^2} \frac{1}{V} \right] dV = - \frac{g_0 W_D}{\beta} \int_{\gamma_E}^{\gamma} d\gamma \quad (100)
 \end{aligned}$$

After integrating this equation and manipulating the result, one obtains the following expression for density ratio as a function of velocity:

$$\begin{aligned}
 \gamma = \gamma_E - \frac{\beta \ln \left( \frac{V}{V_E} \right)}{g_0 W_D} \left\{ \frac{1}{2} \frac{L}{D} \ln \left( \frac{V}{V_E} \right) + \right. \\
 \left. \frac{1}{2} \frac{W_V}{W_D} \frac{1}{V_E^2} + \gamma_E \right\} - \\
 \frac{\beta W_V}{4 g_0 V_E^2 W_D^2} \left( \frac{V_E^2}{V^2} - 1 \right) \quad (101)
 \end{aligned}$$

Using eq (93) the deceleration may be found:

$$-\frac{\dot{V}}{g_0} = W_D V^2 \gamma \quad (102)$$

Substituting eq (101) into eq (102),

$$\begin{aligned}
 -\frac{\dot{V}}{g_0} = & \gamma_E V_E^2 W_D \left(\frac{V}{V_E}\right)^2 - \\
 & \frac{\beta}{g_0} \left(\frac{V}{V_E}\right)^2 \ln\left(\frac{V}{V_E}\right) \left[ \frac{V_E^2}{2} \frac{L}{D} \ln\left(\frac{V}{V_E}\right) + \right. \\
 & \left. + \frac{1}{2} \frac{W_V}{W_D} + \gamma_E V_E^2 \right] + \\
 & \frac{\beta}{4g_0} \frac{W_V}{W_D} \left[ \left(\frac{V}{V_E}\right)^2 - 1 \right]
 \end{aligned} \tag{103}$$

To find the maximum deceleration one takes

$$\frac{d}{dV} \left( -\frac{\dot{V}}{g_0} \right) = 0 \tag{104}$$

Performing the indicated differentiation on eq (103) and manipulating the result, one obtains:

$$\begin{aligned}
 & \left[ 1 + 2 \ln\left(\frac{V}{V_E}\right) \right] \left[ \gamma_E + \frac{1}{2} \frac{W_V}{W_D} \frac{1}{V_E^2} \right] \\
 & = -\frac{L}{D} \ln\left(\frac{V}{V_E}\right) \left[ 1 + \ln\left(\frac{V}{V_E}\right) \right] + \\
 & \quad \frac{1}{2} \frac{W_V}{W_D} \frac{1}{V_E^2} + 2 \gamma_E W_D
 \end{aligned} \tag{105}$$



where the quantities containing  $\frac{1}{2} \frac{W_y}{W_p} \frac{1}{V_E^2}$  and  $y_E$  may be taken as negligible compared to the other terms (see Appendix B). One therefore obtains the equation

$$\left[ \ln \left( \frac{V}{V_E} \right) \right]^2 + \left( 1 + \frac{2\gamma_E}{L/D} \right) \left[ \ln \left( \frac{V}{V_E} \right) \right] + \frac{\gamma_E}{L/D} = 0 \quad (106)$$

Completing the square,

$$\left[ \ln \left( \frac{V}{V_E} \right) + \left( \frac{1}{2} + \frac{\gamma_E}{L/D} \right) \right]^2 = \frac{1}{4} + \left( \frac{\gamma_E}{L/D} \right)^2 \quad (107)$$

solving for the velocity

$$V_m = V_E \exp \left\{ - \left[ \frac{1}{4} + \left( \frac{\gamma_E}{L/D} \right)^2 \right]^{1/2} - \left( \frac{1}{2} + \frac{\gamma_E}{L/D} \right) \right\} \quad (108)$$

where the minus sign is taken on the radical since  $V$  must always be less than  $V_E$ . Letting

$$K_1 = - \left[ \frac{1}{4} + \left( \frac{\gamma_E}{L/D} \right)^2 \right]^{1/2} - \left( \frac{1}{2} + \frac{\gamma_E}{L/D} \right) \quad (109)$$

and substituting eq (109) into eq (103), one obtains the following expression for the maximum deceleration:

$$\begin{aligned} \left(-\frac{\dot{V}}{g_0}\right)_m &= \gamma_E V_E^2 W_D \exp(2K_1) - \\ &\quad \frac{K_1 \beta}{g_0} \exp(2K_1) \left[ \frac{V_E^2}{2} \frac{L}{D} K_1 + \right. \\ &\quad \left. \frac{1}{2} \frac{W_V}{W_D} + \gamma_E V_E^2 \right] + \\ &\quad \frac{\beta}{4g_0} \frac{W_V}{W_D} \left[ \exp(2K_1) - 1 \right] \quad (110) \end{aligned}$$

The altitude at which maximum deceleration occurs can be found by substituting eq (109) into (101):

$$\begin{aligned} \gamma_m &= \gamma_E - \frac{\beta K_1}{g_0 W_D} \left[ \frac{1}{2} \frac{L}{D} K_1 + \right. \\ &\quad \left. \frac{1}{2} \frac{W_V}{W_D} \frac{1}{V_E^2} + \gamma_E \right] - \\ &\quad \frac{\beta W_V}{4 V_E^2 g_0} \frac{1}{W_D^2} \left[ \exp(-2K_1) - 1 \right] \quad (111) \end{aligned}$$

The preceding analysis covers gliding entry from circular orbital speeds for flight-path angles up to approximately 15 degrees. In the following analysis, this solution will

be extended to cover gliding entry at supercircular speeds at small flight-path angles.

Gliding Entry at Supercircular Speeds at Small Entry Angles With Constant Lift-Drag Ratio. Wang and Ting have described a method for extending the analysis for gliding entry at small flight-path angles to supercircular entry (ref 43:565-566). This method will be applied in the following analysis. The assumptions are:

$$1. \frac{L}{D} > 0$$

$$2. (mg + B_F) \sin \gamma \ll D$$

$$3. \text{ For small } \gamma : \sin \gamma \cong \gamma ; \cos \gamma \cong 1$$

4.  $V \cong V_E$ . This assumption has been shown to be valid for the initial phases of entry up to maximum deceleration (refs 16:77; 26;43:565). This is the region of interest in this analysis. That is, the effect of buoyancy on maximum deceleration, velocity, and altitude of maximum deceleration is desired.

The basic equations of motion, eqs (62) to (65) become:

$$\dot{V} = -g_0 W_D \gamma V^2 \quad (112)$$

$$V \dot{\gamma} = -g_0 \frac{L}{D} W_D \gamma V^2 - g_0 W_V \gamma + g_0 - \frac{V^2}{R_F} \quad (113)$$

$$\dot{h} = -V \gamma \quad (114)$$

One may also write

$$\dot{V} = \frac{dV}{dy} \dot{y} \quad (115)$$

and

$$\dot{y} = \beta V \gamma y \quad (116)$$

Eq (116) is obtained from eqs (48) and (114). From eqs (112), (115), and (116), one has that

$$\frac{dV}{V} = -\frac{g_0 W_D}{\beta \gamma} dy \quad (117)$$

One may also write

$$V \dot{\gamma} = V \dot{V} \frac{d\gamma}{dV} = -g_0 \frac{L}{D} W_D V^2 \gamma - g_0 W_V \gamma + g_0 - \frac{V^2}{R_P} \quad (118)$$

where eq (113) and the chain rule have been used.

Substituting eqs (115) and (116) into eq (118) one obtains

$$\int_{\gamma_E}^{\gamma} \gamma d\gamma = -\frac{g_0}{\beta} \left( W_D \frac{L}{D} + \frac{W_V}{V_E^2} \right) \int_{\gamma_E}^{\gamma} dy + \frac{1}{R_P \beta} \left( \frac{g_0 R_P}{V_E^2} - 1 \right) \int_{\gamma_E}^{\gamma} \frac{dy}{\rho} \quad (119)$$

Upon integration this becomes

$$\gamma = \left[ \gamma_E^2 + K_2 (\gamma - \gamma_E) + K_3 \ln\left(\frac{\gamma}{\gamma_E}\right) \right]^{1/2} \quad (120)$$

where

$$K_2 = -\frac{2g_0}{\beta} \left( W_D \frac{L}{D} + \frac{W_V}{V_E^2} \right) \quad (121)$$

$$K_3 = \frac{2}{R_p \beta} \left( \frac{g_0 R_p}{V_E^2} - 1 \right) \quad (122)$$

By substituting eq (120) into (eq (117) velocity can be found as a function of density ratio, hence of altitude:

$$\frac{dV}{V} = -\frac{g_0 W_D}{\beta} \frac{d\gamma}{\gamma(y)} \quad (123)$$

The integral in eq (123) can be evaluated by substituting eq (120) for  $\gamma(y)$ . The integral has  $\gamma(y)$  in the denominator and thus depends on the minimum value of  $\gamma(y)$ . The minimum value of  $\gamma(y)$  occurs at the point of maximum deceleration (ref 43:565).

$$\gamma = \gamma_m \quad \text{at} \quad \gamma(y) = \gamma(y)_{\min} \quad (124)$$

The term  $\ln\left(\frac{y}{y_E}\right)$  is therefore expanded into a Taylor's series around the point  $y = y_m$  as follows:

$$\ln\left(\frac{y}{y_E}\right) = \ln\left(\frac{y_m}{y_E}\right) + \frac{1}{y_m} \frac{(y - y_m)}{1!} - \frac{1}{y_m^2} \frac{(y - y_m)^2}{2!} + \dots \quad (125)$$

By retaining only the first three terms in the expansion, eq (120) can be written in the form

$$\gamma = a_2 y^2 + b_2 y + c_2 \quad (126)$$

where

$$a_2 = \frac{-K_3}{2y_m^2} = \frac{1}{y_m^2 \beta R_P} \left( 1 - \frac{g_0 R_P}{V_E^2} \right) \quad (127)$$

$$b_2 = K_2 + \frac{2K_3}{y_m} \quad (128)$$

$$\text{or } b_2 = \frac{4(g_0 R_p - V_E^2)}{y_m \beta R_p V_E^2} - \frac{2g_0}{\beta} \left( w_D \frac{L}{D} + \frac{W_V}{V^2} \right) \quad (128a)$$

$$C_2 = y_E^2 - K_2 y_E + \frac{K_3}{2} \left[ 2 \ln \left( \frac{y_m}{y_E} \right) - 3 \right] \quad (129)$$

$$\text{or } C_2 = y_E^2 + \frac{2g_0 y_E}{\beta} + \frac{(g_0 R_p - V_E^2)}{\beta R_p V_E^2} \left[ 2 \ln \left( \frac{y_m}{y_E} \right) - 3 \right] \quad (129a)$$

The coefficient  $a_2$  is seen to be greater than one because  $g_0 R_p < V_E^2$  for supercircular entry. Eq (123) thus has the form

$$\int_{V_E}^V \frac{dV}{V} = \int_{y_E}^y \frac{dy}{(a_2 y^2 + b_2 y + c_2)^{1/2}} \quad (130)$$

which may be integrated (for example, see ref 44:70, #162) to yield

$$\ln\left(\frac{V}{V_0}\right) = \frac{-g_0 W_D}{\beta a_2^{1/2}} \times \ln \left[ \frac{2a_2 y + b_2 + 2a_2^{1/2}(a_2 y^2 + b_2 y + c_2)^{1/2}}{2a_2 y_0 + b_2 + 2a_2^{1/2}(a_2 y_0^2 + b_2 y_0 + c_2)^{1/2}} \right] \quad (131)$$

It was stated previously that the minimum value of  $\gamma(y)$  occurs when  $y$  is equal to  $y_m$ . This is obtained as follows. The magnitude of the deceleration vector felt by an accelerometer aboard the vehicle (see ref 26:635) is

$$G = \left[ \left( \frac{L + B_F}{W} \right)^2 + \left( \frac{D}{W} \right)^2 \right]^{1/2} \quad (132)$$

for small angles  $\gamma$ . Manipulating eq (132), one obtains

$$G \cong W_D y V^2 \left[ 1 + \left( \frac{L}{D} \right)^2 \right]^{1/2} \quad (133)$$

Maximum  $G$  is experienced when  $yV^2$  is a maximum, or when

$$\frac{d}{dt}(yV^2) = 0 \quad (134)$$

Performing the differentiation of eq (134),

$$2yV\dot{V} + V^2\dot{y} = \frac{d}{dt}(yV^2) \quad (135)$$



Substituting eqs (49) and (112) into eq (135) one obtains

$$\frac{d}{dt}(y v^2) = y v^3 (\beta \gamma - 2 y g_0 W_0) \quad (136)$$

Substituting eq (134) into eq (136),

$$\gamma_m = \frac{2 g_0 W_0}{\beta} y_m \quad (137)$$

Since  $y$  equals  $e^{-\beta h}$  one sees immediately that the larger  $y$  gets the smaller is  $\gamma$ . Since this analysis is concerned with the trajectory only up to the point of maximum deceleration, one sees that  $\gamma_{min}$  occurs at  $y_m$ . Eqs (120) and (137) give the density ratio and flight-path angle at maximum deceleration. With the value for  $y_m$  inserted into eq (131), the velocity as a function of altitude is known.

The preceding analysis gives excellent results for the non-buoyant entry case (ref 43:566). The next section will treat equilibrium gliding entry.

Equilibrium Gliding Entry at Small Flight-Path Angles With Constant Lift-Drag Ratio. This entry mode has been studied extensively by many authors (refs 16, 17, 19, 24

28,45). An equilibrium glide trajectory is characterized by the balance between the weight and the sum of the lift, buoyant, and centrifugal forces at each point along the shallow path (refs 19:20; 45: chapter 10 page 2). For this type of entry the following assumptions are made:

$$1. (mg - B_F) \sin \gamma \ll D$$

$$2. L > 0 \text{ for } V_E < V_{c,IR} \text{ and } L < 0 \text{ for } V_E > V_{c,IR}. \text{ This}$$

is evident from the definition of circular orbital speed and the equilibrium glide trajectory. At circular orbital speed, the centrifugal force is equal to the weight. If the velocity is greater than circular orbital velocity, then the centrifugal force is greater than the weight and the lift must act down to keep the balance of forces equal (ref 45: chapter 10, page 10:24).

3. For the small, slowly-changing path angles involved,  $\dot{\gamma} \cong 0$ . This assumption is valid as long as  $\gamma$  remains small. Computer studies for the non-buoyant entry case have indicated that  $\gamma$  remains less than one degree for about 97% of the trajectory (ref 46:6; also see ref 19:20).

$$4. \text{ For small } \gamma: \sin \gamma \cong \gamma; \cos \gamma \cong 1.$$

With these assumptions the basic equations of motion, eqs (62)-(65), become:

$$\dot{V} = -g_0 W_D \gamma V^2 \quad (138)$$

$$g_0 \frac{L}{D} W_D \gamma V^2 + \frac{V^2}{r} = g_0 (1 - W_V \gamma) \quad (139)$$

$$\dot{r} = -V \gamma \quad (140)$$

The velocity variation as a function of altitude may be found directly from eq (139):

$$V = \frac{(g_0 R_P)^{1/2} (1 - W_V y)^{1/2}}{(1 + g_0 R_P \frac{L}{D} W_D y)^{1/2}} \quad (141)$$

Inserting eq (141) into eq (138), the deceleration at any point in the trajectory is found:

$$-\frac{\dot{V}}{g_0} = W_D g_0 R_P \left( \frac{1 - W_V y}{1 + g_0 R_P \frac{L}{D} W_D y} \right) y \quad (142)$$

To find the maximum deceleration, the following condition is applied:

$$\frac{d}{dy} \left( -\frac{\dot{V}}{g_0} \right) = 0 \quad (143)$$

Performing the indicated differentiation of eq (142) and applying eq (143), one obtains

$$a_3 y_m^2 + b_3 y_m - 1 = 0 \quad (144)$$

where

$$a_3 = g_0 R_P \frac{L}{D} W_D W_V \quad (145)$$

$$b_3 = 2 W_V \quad (146)$$

Solving eq (144)

$$y_m = \frac{-1 \pm \left(1 + g_0 R_P \frac{L}{D} \frac{W_D}{W_V}\right)^{1/2}}{g_0 R_P \frac{L}{D} W_D} \quad (147)$$

Since the quantity  $g_0 R_P$  is very large compared to one, eq (147) may be written

$$y_m \cong \frac{1}{\left(g_0 R_P \frac{L}{D} W_D W_V\right)^{1/2}} \quad (148)$$

Substituting eq (148) into eq (142), one obtains, after manipulation, an expression for maximum deceleration:

$$\left(\frac{\dot{v}}{g_0}\right)_m = \frac{1}{L/D} \left\{ \frac{(g_0 R_P)^{1/2} \left(\frac{W_D}{W_V} \frac{L}{D}\right)^{1/2} - 1}{(g_0 R_P)^{1/2} \left(\frac{W_D}{W_V} \frac{L}{D}\right)^{1/2} + 1} \right\} \quad (149)$$

It is interesting to note that no maximum deceleration occurs during the equilibrium glide descent of a non-buoyant vehicle, whereas it does in the buoyant case. In the non-buoyant case, the deceleration increases continuously during the glide, asymptotically approaching the value

$$\left(-\frac{\dot{V}}{g_0}\right)_m = \frac{1}{L/D} \quad (149a)$$

and is dependant only on the lift-drag ratio (ref 19:21,22). In the buoyant case, it is seen that the maximum deceleration depends on the gravitational characteristics and size of the planet, and on the vehicle drag and size. The maximum deceleration for the two cases varies according to the term in the brackets in eq (149).

The flight-path angle changes continuously during the descent, as the vehicle "hunts" for the equilibrium position (ref 19:6). To find an expression for flight-path angle as a function of altitude, eq (139) is differentiated with respect to time to yield

$$\frac{2V\dot{V}}{g_0 R_p} \left(1 + g_0 R_p \frac{L}{D} W_D \gamma\right) + \frac{V^2}{g_0 R_p} \left(g_0 R_p \frac{L}{D} W_D \dot{\gamma}\right) = -W_V \dot{\gamma} \quad (150)$$

But

$$\dot{y} = \beta V \gamma y \quad (151)$$

$$\dot{V} = -g_0 W_D \gamma V^2 \quad (152)$$

Inserting eqs (151) and (152) into eq (150), one obtains after manipulation that

$$\gamma = \frac{2}{R_P \beta \left( \frac{L}{D} + \frac{1}{g_0 R_P} \frac{W_V}{W_D} \right)} \times (a_4 y^2 + b_4 y + c_4) \quad (153)$$

where

$$a_4 = g_0 R_P \frac{L}{D} W_D W_V \quad (154)$$

$$b_4 = W_V - g_0 R_P \frac{L}{D} W_D \quad (155)$$

$$c_4 = -1 \quad (156)$$

To find the range of the glide vehicle, the following analysis applies. The range is defined by

$$RANGE \equiv R_g = \int_{t_r}^t V_{\theta} dt \quad (157)$$

Since  $V_{\theta} = -V \cos \gamma \cong -V$ ,

$$R_g = - \int_{t_r}^t V dt \quad (158)$$

The following transformation is made:

$$dt = \frac{dy}{\dot{y}} \quad (159)$$

or using eq (151),

$$dt = \frac{-dy}{\beta y V \gamma} \quad (160)$$

Substituting eq (160) into eq (158),

$$R_g = \frac{1}{\beta} \int_{y_E}^y \frac{dy}{y \gamma(y)} \quad (161)$$

The flight-path angle as a function of  $y$  is given by eq (153). Substituting this expression into eq (161)

$$R_g = a_5 \int_{y_E}^y \frac{dy}{y(a_4 y^2 + b_4 y + c_4)} \quad (162)$$

where  $a_4$ ,  $b_4$ , &  $c_4$  are given by eqs (154) to (156), and where

$$a_5 = \frac{R_p}{2} \left( \frac{L}{D} + \frac{1}{g_0 R_p} \frac{W_v}{W_D} \right) \quad (163)$$

When it is noted that

$$b_4^2 > 4 a_4 c_4 \quad (164)$$

eq (162) can be evaluated (ref 44:69,70;#151,158). Performing the integration and manipulating the result, one obtains:



$$R_g = a_5 \frac{1}{2} \frac{b_4}{b_5} \times$$

$$\ln \left[ \frac{\frac{W_v y + 1}{g_0 R_P \frac{L}{D} W_D y + 1}}{\frac{W_v y_E + 1}{g_0 R_P \frac{L}{D} W_D y_E + 1}} \right] - \frac{1}{2} \ln \left[ \frac{\frac{y^2}{a_4 y^2 + b_4 y - 1}}{\frac{y_E^2}{a_4 y_E^2 + b_4 y_E - 1}} \right] \quad (165)$$

where

$$b_5 = W_v + g_0 R_P \frac{L}{D} W_D \quad (166)$$

and the other constants are as previously defined.

The preceding analyses were concerned with deriving expressions which show the effect of buoyancy on the initial stages of entry. The next section will analyze the terminal dynamics.

#### Terminal Dynamics

At some point in the entry trajectory, the entering vehicle passes to subsonic speeds and begins a terminal

velocity descent. The previous analytic solutions are valid only for the initial phases of entry. Moe (ref 47; 50-53) gives an analytic approximation for determining the trajectory of a vehicle as it "bends over" into the vertical terminal descent. In the following analysis it is assumed that the vehicle is in its terminal descent, and that the aerodynamic lift is zero. Figure 4 shows the coordinate system used. From the figure, the rate of change of momentum in the  $x$  direction is

$$+\frac{d}{dt}(m V_x) = D \cos \gamma \quad (167)$$

The rate of change of momentum in the  $z$  direction is

$$+\frac{d}{dt}(m V_z) = D \sin \gamma + B_F - m g_0 \quad (168)$$

Since the vehicle is not subject to control in the horizontal direction, this analysis will only be concerned with eq (168). In this terminal phase of the entry,  $\gamma \cong \frac{\pi}{2}$  so that  $\sin \gamma \cong 1$  (refs 16:81; 48:148; 49:7). Introducing this assumption and eqs (53) and (56) into eq (168),

$$\dot{V}_z = +\frac{C_D S}{m} \frac{\rho_0}{2} \gamma V^2 + \frac{\rho_0 B_V g_0}{m} \gamma - g_0 \quad (169)$$

If the vehicle is assumed to be spherical in shape, eq (169) becomes

$$\dot{V}_z = + \frac{C_D \rho_0}{2m} \left( \frac{\pi d^2}{4} \right) y V^2 + \frac{\rho_0 g_0}{m} \left( \frac{\pi d^3}{6} \right) y - g_0 \quad (170)$$

Time may be eliminated from eq (170) by the following transformation

$$\dot{V}_z = \frac{dV_z}{dy} y = -\beta y V_z \frac{dV_z}{dy} \quad (171)$$

Substituting eq (171) into eq (170)

$$\frac{dV_z^2}{dy} + \frac{C_D \rho_0}{\beta m} \left( \frac{\pi d^2}{4} \right) V^2 = \frac{2g_0}{\beta y} - \frac{\rho_0 g_0}{\beta m} \left( \frac{\pi d^3}{3} \right) \quad (172)$$

Schlichting and others have shown that the drag coefficient varies strongly with Reynold's number (refs 50:15-16; 51:179-181). For a sphere at high Reynold's number

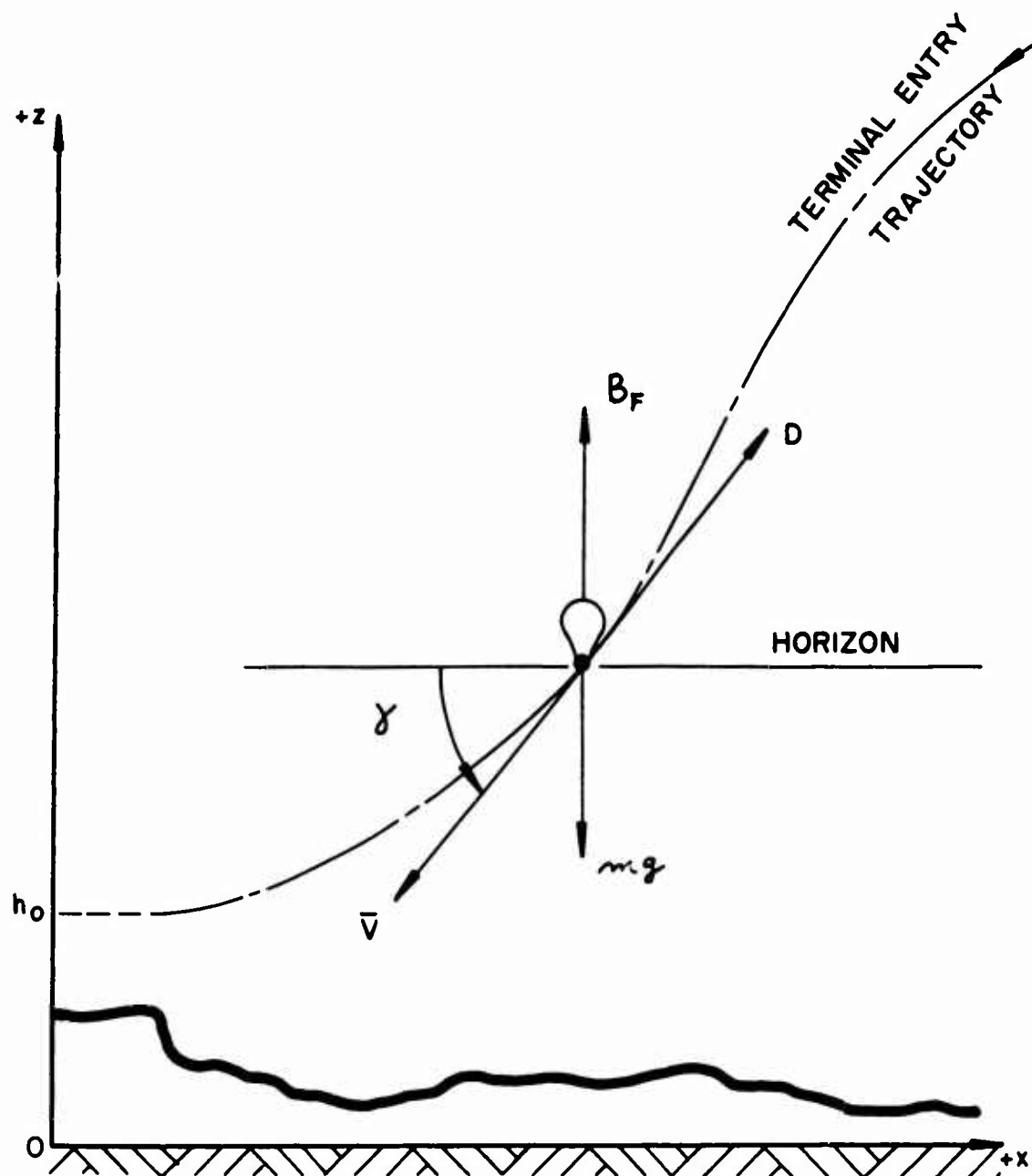


Fig. 4

Coordinate System for Terminal  
Descent of Buoyant Planetary  
Entry Vehicle

(above the critical value) the drag coefficient is quite small: on the order of 0.1. As the Reynold's number decreases, the drag coefficient increases and reaches a theoretical value of over 200 at a Reynold's number of 0.1 (refs 50:16; 52:593). Fortunately, however, the drag coefficient is nearly constant at a value of about 0.45 from a Reynold's number of 300 to the critical value. The critical value of Reynold's number for a sphere is given as  $3.85 \times 10^5$  (ref 50:470). Therefore, in this approximate analysis, the drag coefficient is assumed constant at a value of 0.45. If the diameter of the buoyant volume is assumed constant, eq (172) becomes

$$\frac{dV_z^2}{dy} + K_4 V_z^2 = K_5 + \frac{K_6}{y} \quad (173)$$

where

$$K_4 = 0.353 \frac{\rho_0 d^2}{\beta m} \quad (174)$$

$$K_5 = -1.047 \frac{\rho_0 g_0 d^3}{\beta m} \quad (175)$$

$$K_6 = \frac{2 g_0}{\beta} \quad (176)$$

The drag coefficient , instead of being considered constant throughout the whole range of Reynold's numbers encountered, may be taken as piecewise constant over certain small increments of distance. The same holds for density. The mass term in these constants must be considered in greater detail. The mass consists of three parts:

$$m = m_s + m_a + m_g \quad (177)$$

where  $m_s$  is the structural mass of the body,  $m_a$  is the apparent mass of ambient air affected by the body, and  $m_g$  is the mass of the gas inside the buoyant volume. This representation assumes that the balloon and its contained gas move as a rigid body (ref 53:5). For a spherical balloon, the apparent mass is (ref 53:5):

$$m_a = 0.5 \rho_{\text{ATM}} \frac{\pi d^3}{6} \quad (178)$$

The mass of the gas contained by the balloon is:

$$m_g = \rho_g \frac{\pi d^3}{6} \quad (179)$$

The pressure and temperature of the gas inside the buoyant cell will in general be greater than that of the ambient air, due to the entry heating.

The apparent mass given in eq (178) is usually considered negligible. This is valid at high altitudes (and should thereby be valid for Mars) but could be significant for Venus, where the atmosphere may exceed that of Earth by several orders of magnitude.

With these considerations, eq (173) may be integrated subject to the boundary condition,

$$V_z(y_1) = V_{z1} \quad (180)$$

to find the solution

$$V_z^2 = \frac{K_5}{K_4} + \int \frac{K_6}{y} e^{K_4 y} dy \cdot e^{-K_4 y} \cdot C e^{-K_4 y} \quad (181)$$

where  $C$  is a constant, found from eq (180).

The boundary condition given in eq (180) is found from one of the analytic solutions of the previous sections. With an expression for  $V_z$  as a function of  $y$  as given by eq (181) one may determine the required diameter of buoyant volume necessary to bring the vehicle to zero vertical velocity at a specified distance  $h_0$  above the ground. This condition is given by

$$V_z(y_0) = 0 \quad (182)$$

If gas is not released, the vehicle will then rise until its equilibrium floating altitude is reached.

After the balloon has reached equilibrium floating conditions, the drag coefficient can be taken as 0.1, the super-critical Reynold's number value. Schlichting has shown (ref 50:38) that a supercritical flow pattern can be achieved by mounting a thin "tripping wire" around the equator of the sphere perpendicular to the flow. (also see refs 52:592 and 53:14).

Linnell has given a more complete solution to the vertical entry (ref 66:329-330) in which he uses piecewise-constant drag coefficients and piecewise-exponential atmospheres. His solution cannot be evaluated in closed form and a numerical approach must be used.

### Discussion of Results

It can be easily seen from an examination of the entry dynamics equations that buoyancy has a negligible effect on velocity, altitude of maximum deceleration, and maximum deceleration. When curves were being prepared, it was obvious that this was going to be the case. A small divergence from the case of entry with no buoyancy begins to be noticeable at altitudes below the altitude of maximum deceleration. However, this is not in the area of interest. Further, at lower altitudes where buoyancy does begin to have some noticeable effect, the assumptions made in deriving the analytic solutions are not entirely valid.



Therefore, the results reduce to the case of entry without buoyancy. These results have been well plotted and tabulated and will not be reproduced here.

However, there is one case for which the buoyant effect is not entirely insignificant, and that is the case of equilibrium-gliding entry. The results for this entry mode show that maximum decelerations for small lift-drag ratios of 0.01 and buoyant diameters of 300 ft. are reduced about 8% for Mars entry and about 6% for Venus entry. For lift-drag ratios of 1.0, these percentage decrease in maximum deceleration are 1.1% for Mars and 0.7% for Venus. These results are shown in figures 5 and 6 for Mars and Venus, respectively, using eq (149). The drag coefficient was assumed constant at a value of 2.2 for both Mars and Venus. It is interesting to note that the maximum deceleration for equilibrium-gliding entry does not depend on the mass of the entering vehicle, but only on the circular orbital speed of the planet, the lift-drag ratio, and the diameter of the buoyant volume.

Eqs (180) - (182) were used to find the diameter of balloon required to decelerate a 500 pound payload to zero vertical velocity at 30,000 ft for a Venus equilibrium-glide entry. The lift-drag ratio was assumed 1.0 and the drag-weight parameter was taken to be 5.0. Using helium for the buoyant gas and a balloon skin of aluminized mylar, the balloon diameter was calculated to be 13 ft. For Mars, payloads would be on the order of 50 - 100 pounds for balloon diameters of 150 - 200 ft for "soft" landings. Auxiliary drag devices and short rocket bursts just before landing may be required.

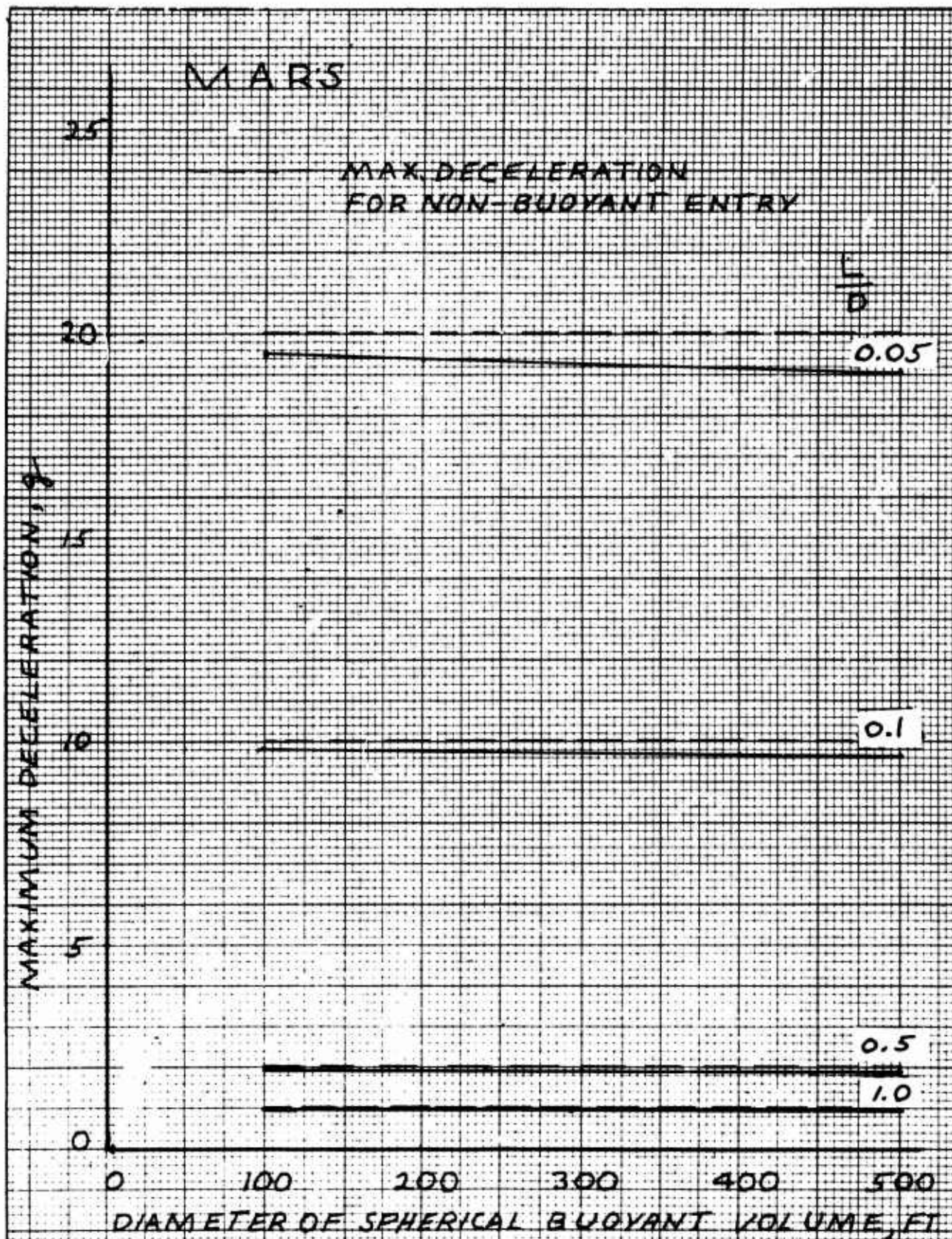
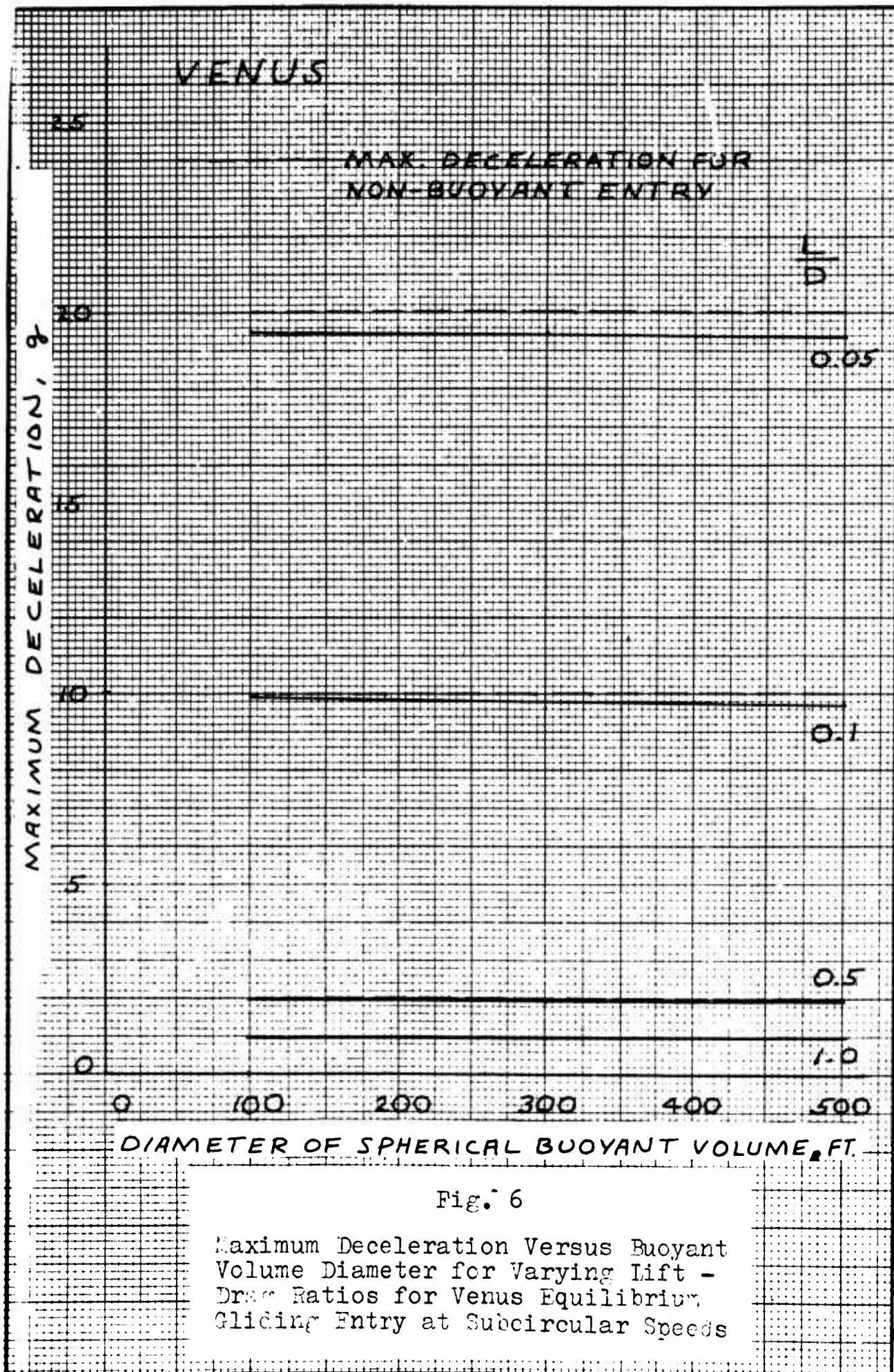


Fig. 5

Maximum Deceleration Versus Buoyant  
Volume Diameter for Varying Lift-  
Drag Ratios for Mars Equilibrium  
Gliding Entry at Subcircular Speeds



### III. Gasdynamic Heating

This chapter contains a generalized discussion of the heating effects of buoyant planetary entry. Several methods of solving the heat problem are discussed.

#### General

It is beyond the scope of this study to attempt a detailed analysis of this complex problem. However, certain considerations can be made based on the equations previously derived and the studies of others.

Entry Heating. When a vehicle enters a planetary atmosphere, it converts its kinetic and potential energy into heat energy which heats the surrounding atmosphere. Some of this energy is transferred to the surface of the vehicle. The amount of energy so transferred can be expressed as a fraction of the vehicle's total energy.

At high altitudes, as much as one-half of the vehicle's lost energy can appear as heat in the body (ref 18:36). The rate of heat input to an entry vehicle can be written as (ref 54:3):

$$\dot{H} = \frac{1}{2} C_H \rho S V^3 \quad (183)$$



Where  $C_H$  is the total overall heat transfer coefficient. The heating rate thus is seen to depend on the cube of the velocity. This means that a reduction in velocity of 1% is equivalent to a heating rate of reduction of 3% if the velocity is initially 20,000 fps. A gross analysis may now be performed to determine the maximum effect of buoyancy on the velocity of an entry vehicle.

Effect of Buoyancy. The greatest effect of buoyancy on velocity will obviously be for the radial entry case where the buoyant force vector acts oppositely to the velocity vector. From eq (85) for the vertical entry case, it is seen that the gross effect of buoyancy is to decrease the velocity by a factor of  $\left(\frac{W_V}{W_D}\right)^{1/2}$  from the non-buoyant case. For a Mars entry vehicle of 20,000 lbs. and a buoyant volume diameter of 200 feet, it was calculated that the effect of buoyancy is to decrease the velocity at the point of maximum deceleration by about 0.5% for entry speeds of 15,000 fps. This corresponds to a decrease in the heating rate of about 1.75%, due to buoyancy alone. Thus, it is immediately seen that buoyancy alone cannot solve the heating problem. Further, although buoyancy has its greatest effect in retarding velocities for the vertical entry case, maximum heating and temperatures also occur for this type of entry (ref 19:38).

Gazley (ref 17:28-29;51) presents data which seems to indicate that the only hope of successful entry for thin-skinned vehicles such as proposed in this study is

entry by orbital decay. In this case, the effect of buoyancy would be negligible since the buoyant force vector is nearly perpendicular to the velocity and is very small at high altitudes. However, it can be seen from figure 19 in Gazley's study (ref 17:51) that the larger the parameter  $\frac{C_D S}{W}$  is, the lower the maximum surface temperature will be. For thin-skinned vehicles such as proposed in this study,  $\frac{C_D S}{W}$  can be on the order of 5-10, for diameters of 250 ft. or greater.

Entry by Orbital Decay. Gazley has pointed out (ref 17:28-29) that in many cases of gradual entry essentially all of the heating can be dissipated from the vehicle skin by radiation. The skin attains the "radiation-equilibrium" temperature where the skin is hot enough to re-radiate the heat caused by kinetic heating. In this case, the maximum surface temperature occurs when the heating rate is a maximum. Gazley gives the equation for maximum surface temperature as (ref 17:29)

$$T_{MAX} = \left[ \frac{\rho_0 (g_0 R_p)^{3/2} \frac{S}{A_S} \dot{H}_{MAX}}{\epsilon \sigma_B (d)^{1/2} \left( \frac{R_e}{M_d} \right)^{1/2} \left( \frac{C_D S}{W} \frac{\rho_0}{2\beta} \right)^{1/2}} \right]^{1/4} \quad (184)$$

Where  $d$  is the hemispherical nose diameter and the other symbols are defined in the list of nomenclature. Based on this formula, Gazley has drawn curves which show that

for a  $\frac{C_D S}{W}$  equal to 0.1,  $d=2\text{ft}$ , and  $\epsilon=0.8$  for a sphere entering the atmosphere of Mars by orbital decay, the maximum stagnation temperature is about 1700R. This graph is reproduced in figure 7 of this study. If the sphere were spinning, the maximum surface temperature would be about 1200R. The important thing here is that eq (184) is seen to depend on  $(d)^{-1/8}$ . Therefore, if it is postulated that the diameter of the spinning sphere is on the order of 250 ft. in diameter it is quickly seen that the maximum equilibrium surface temperatures given in Gazley's curves are roughly halved. For the above described vehicle, therefore, the maximum temperature is about 600R. This is for orbital decay without lift. For a similar entry into the atmosphere of Earth for a spinning sphere, the values for maximum temperature are 2300 R for a 2ft. diameter and 1150 R for a 250ft. diameter. The values for Venus are roughly the same as those for Earth, or a little less (ref 17:25). If  $\frac{C_D S}{W}$  on the order of 5-10 can be assumed (for example, a 250ft. diameter sphere with a total vehicle weight on the order of 15,000 lbs.), these maximum temperatures can be decreased considerably, as shown by Gazley's graph.

From the above considerations it can be stated that the necessary conditions for successful entry of thin-skinned balloon vehicles are:

1. Entry by orbital decay, with some type of aerodynamic lift, if possible.

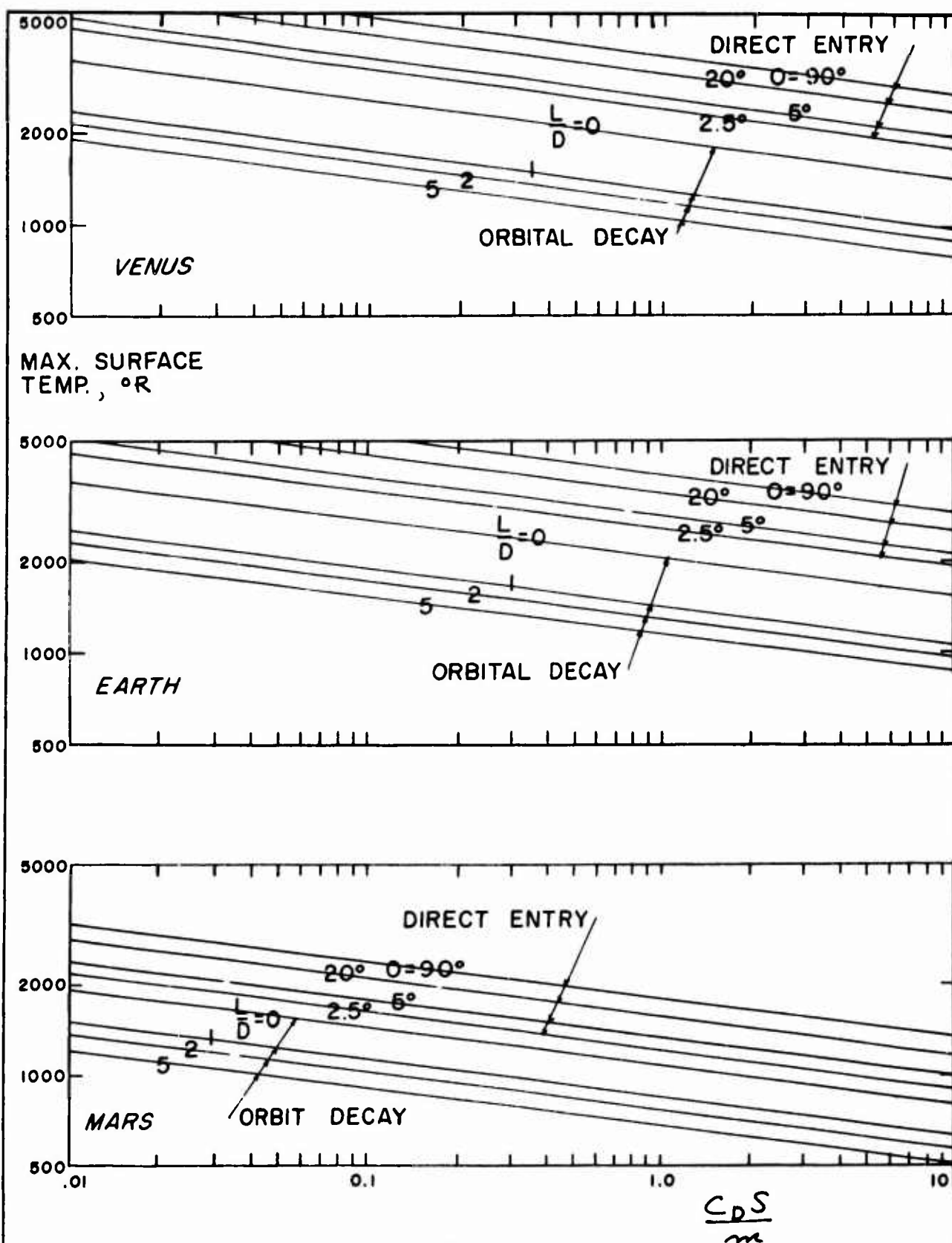


Fig. 7

Maximum Radiation-Equilibrium Surface  
Temperature (°R) Occurring  
During Planetary Entry for a Sphere

(From ref 17: 51)



2. Drag Surface area to weight parameter values on the order of 5-10 or greater.

3. The sphere is an ideal shape because it gives the least surface area for a given volume than other shapes.

4. The sphere must be spinning during entry to avoid stagnation point "hot spots", and decrease local temperatures.

If these conditions can be met, it appears possible that successful entry of balloon-type vehicles into the atmosphere of Venus and Mars can be made without heavy heat-shielding with materials now under development. ( See Chapter IV) .

Other Methods of Heat Alleviation. Nothing has been mentioned in the above considerations about the use of the buoyant gas contained within the buoyant volume as a heat sink or film cooling agent. There would be about  $8 \times 10^6$  cubic feet of gas (probably helium) in a buoyant cell with a diameter of 250 feet. Thus, a large heat sink or film cooling source is available. An interesting report by Robert E. Dannenberg (ref 55) indicates that helium film-cooling a hemisphere at a Mach number of 10 and a stagnation temperature of 8700R was effective in reducing the heat transfer from the high energy stream. The peak heating rate on a hemisphere was reduced considerably. and immediately downstream of the injection port the surface was almost completely insulated from the air flow (ref 55:1).

If the large volume of helium could be used as a heat

sink, the density of the helium could be lowered for a vented balloon. This would increase the vehicle's initial load carrying capability in the planetary atmosphere. As the gas cools, some of the instrumentation for experiments already completed, and whose weight is no longer needed, could be dropped off.

A further system for solving the heat problem, but one which introduces considerable weight and complexity into the system, is the deployable heat shield. Such a heat shield could be deployed and rigidized prior to entry. During entry, it would be ablated or burnt away, bearing the heat load and thus protecting the light buoyant cell (figure 8). Techniques and materials have been developed for the automatic deployment and rigidization of large structures in space (ref 56).

The use of light materials permits packaging of a balloon structure in a small space for later expansion in space. This technique has been successful with the Echo satellite programs, and would permit direct launching from Earth to the target planet. However, one last-resort method can be used if it is desired to launch a buoyant planetary probe and the direct-launch heating problem cannot be solved. This method would be to construct the probe vehicle while in orbit around the Earth, building in the required heat protection, then launch the vehicle from orbit. Undoubtedly, this method would be very expensive. A special type of structure for this application is discussed in the next chapter.

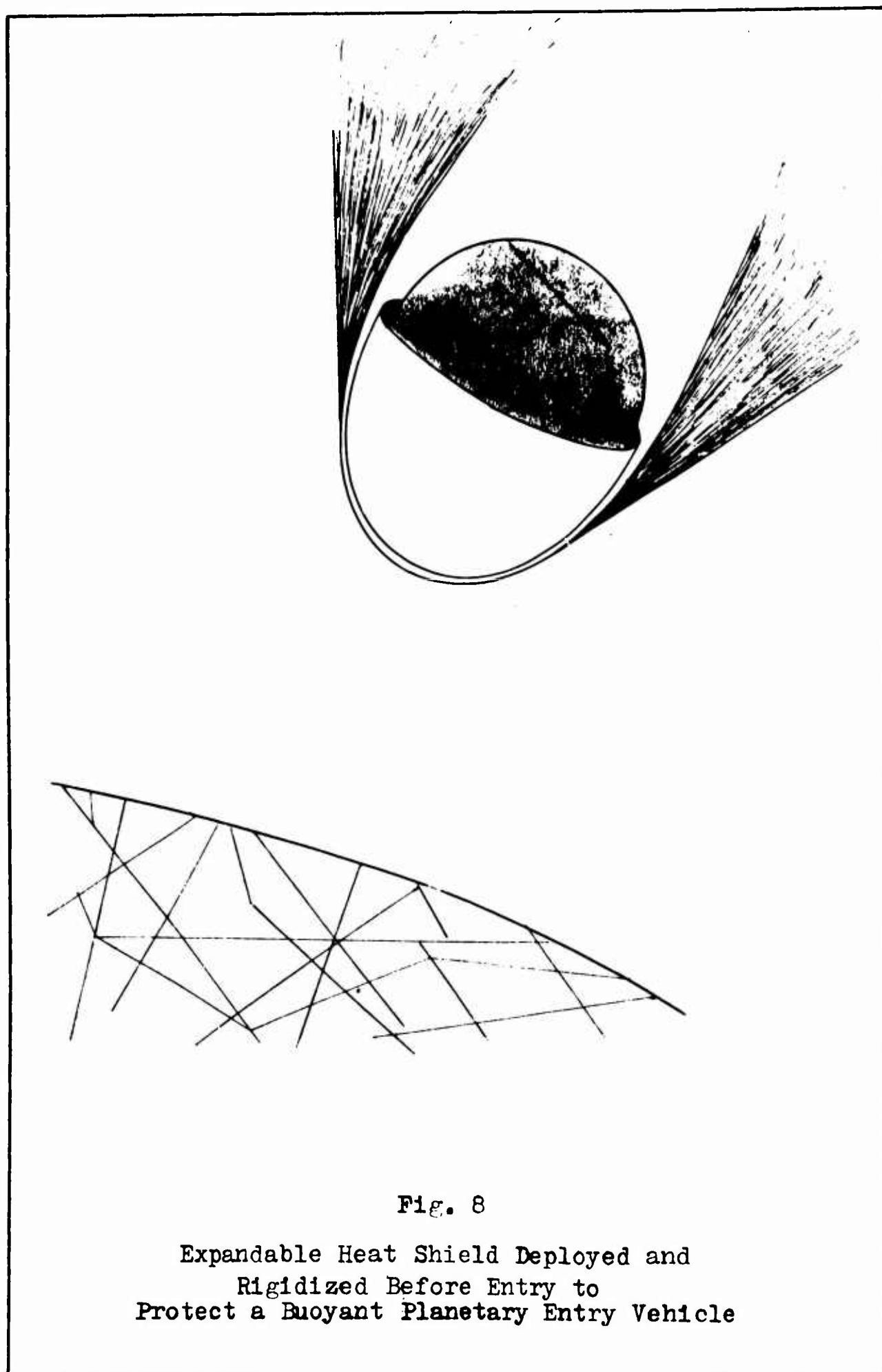


Fig. 8

Expandable Heat Shield Deployed and  
Rigidized Before Entry to  
Protect a Buoyant Planetary Entry Vehicle

#### IV. Materials, Techniques, and Configurations

This chapter contains a discussion of possible materials for the buoyant cell, techniques in accomplishing a mission such as the one proposed in this study, and some possible vehicle configurations.

##### Materials

The first materials considered for the buoyant cell were the same as used in the Echo I and A-12 satellites. The Echo I satellite was made of 0.5 mil thick polyethylene terephthalate plastic film with about 2,200 angstroms of aluminum vapor on the outside surface. (ref 57:7). The Echo A-12 sphere was made of a three-layer laminate of the same type of plastic film used in Echo I sandwiched between two layers of 1080 aluminum foil (ref 58:1). The aluminum vapor and foil serve to protect the film from ultraviolet radiation. Echo I was 100 ft. in diameter when expanded and weighed only 112 lbs. At launch, the whole 100 ft. sphere was folded and packaged into a spherical container only 2.2 ft. in diameter. However, these films have a small permeability to helium which necessitates continuous replenishment of gas for long flights (ref 57:42). These films are so light that it appears they could not be pressurized sufficiently to avoid failure under the high dynamic pressures of entry, without a protecting shield. The same comments apply to research

balloons since most of them are made of polyethylene film also. No new recent films for research balloons have indicated an improvement over polyethylene (ref 13:46). If these types of films are used (almost a necessity in the thin Martian atmosphere due to their light weight) it is anticipated that some sort of heat shield that could later be dropped off will be required for entry.

A second class of materials considered were the new nickel and boron-based fibers under development (ref 59:65). These fibers are designed to withstand the high temperatures of reentry and are being developed for balloon applications (ref 59:65). However, no data could be found on weight.

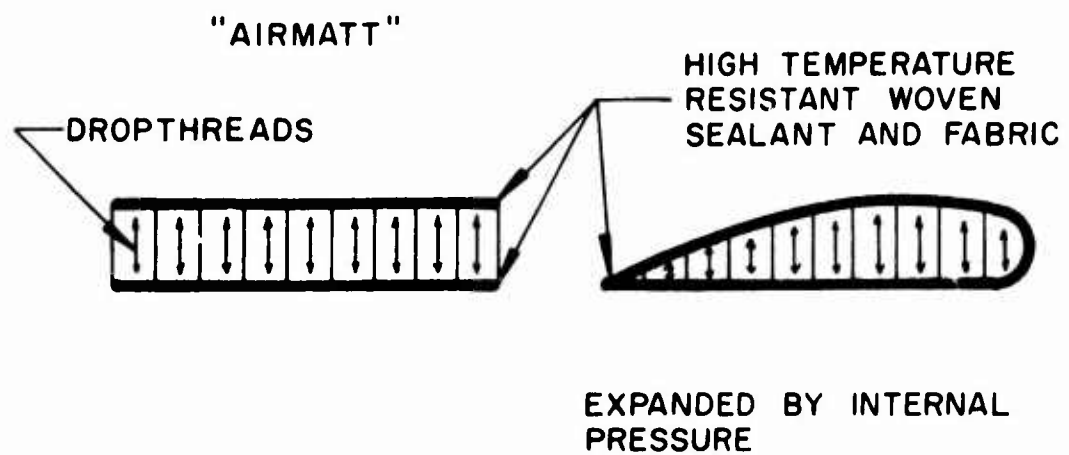
Several particularly promising materials concepts for balloon entry are considered below. Data is taken from reference 59.

1. Airmatt: This is a type of balloon structure that can be packaged in a small space, but when deployed assumes a pre-determined shape, such as an airfoil. This has possible application for the "wings" of an entering buoyant vehicle. For high temperature applications, light metallic-fibers would be used. Another concept involving the use of this material is that an airmatt outer layer could be used to take the entry heat load, then be shed after entry. Figure 9<sub>a</sub> illustrates the airmatt concept.

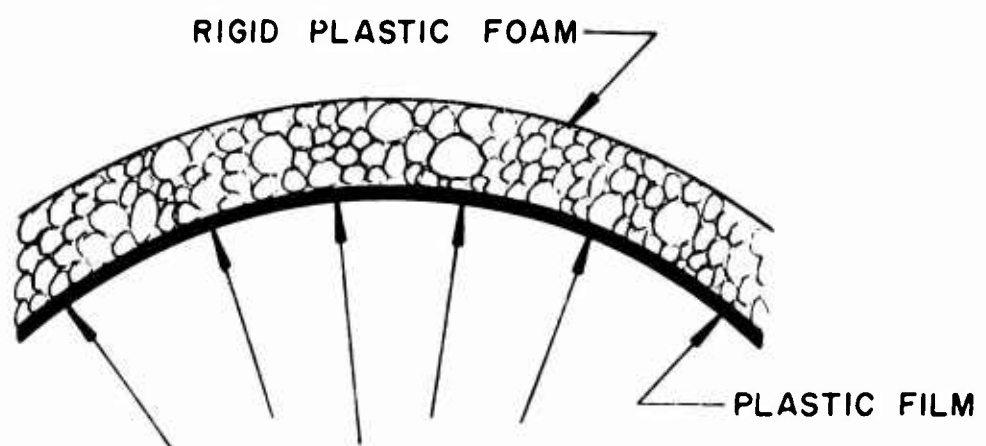
2. Foamed in place: In this application, foam which hardens in space is used to rigidize the outside surface of

a plastic film. This concept could be used for a heat shield for an entry balloon. For example, the foam could be designed to ablate under conditions of entry heating. Figure 9b illustrates the foamed-in-place concept.

3. Drag Cone: An extremely important concept for application to a buoyant entry vehicle, this scheme has been under study by Douglas Aircraft for several years and is explained in reference 56, pages 36-38. As originally conceived this concept was to be used to recover missile boosters. The system consists of an inflatable blunt-body "drag cone" as shown in figure 10, which is reproduced from page 37 of reference 56. This structure is 325 feet in diameter, 226 feet high and weighs about 107,000 lbs. It consists of two sections: an airmatt nose cone section to retain the desired conical shape and capable of withstanding entry temperatures of 1500F. The second section would be a silicone coated fabric. When deployed this section would assume the shape of a large torus and be protected by the airmatt heat shield. Both sections would be packaged in the booster rocket to be recovered. As envisioned by Douglas, the drag cone and booster system would become aerostatically buoyant at an altitude of 2,000 ft. This is accomplished by flowing hydrogen or helium at 400F into the inflated drag cone by means of a combustor-heater handling up to 55 lbs. of gas per second. The vehicle would gradually descend as the bag cools off,



(a) "Airmatt" Expandable Structure



(b) Rigidized Plastic Foam

Fig. 9

"Airmatt" (Douglas Aircraft Co.)  
and Rigid Plastic Foam Concepts

(From ref 59: 63)

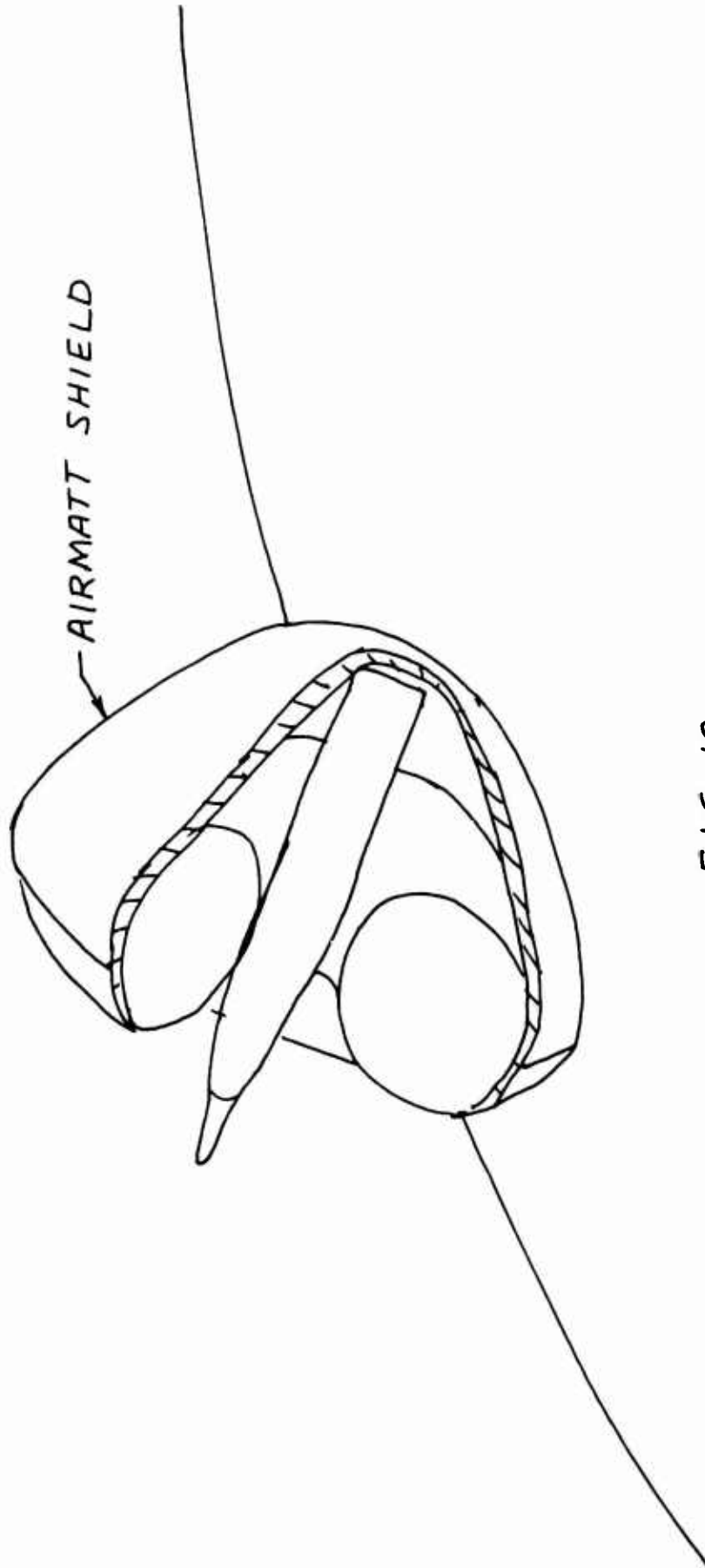


FIG. 10

DOUGLAS AIRCRAFT COMPANY CONCEPT  
FOR BOOSTER RECOVERY DRAG CONE

(FROM REF 56: 37)



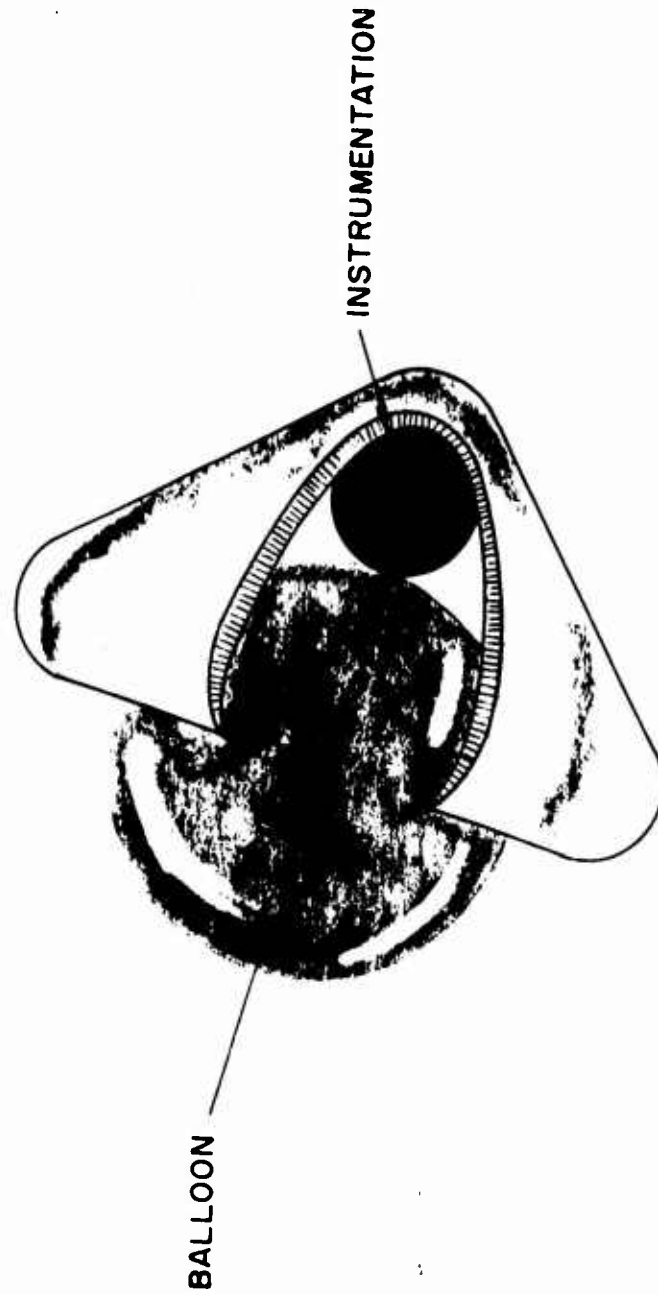


FIG. 11  
"AIRMATT" DRAG CONE PROTECTED BUOYANT  
PLANETARY ENTRY CAPSULE

with an impact speed of no more than 2.5 fps. If the torus is replaced by a lightweight polythelene or other lightweight balloon, this concept could be used to provide heating protection for a buoyant planetary exploration capsule. The airmatt nose-cone would be expendable and be released after the entry is complete. The blunt-conical entry shape has been described as attractive for Venus and Mars entry from a heating standpoint (refs 54;60:10-11; 61).

#### Tension Shell Structure

In the previous chapter it was mentioned that a buoyant planetary probe could be constructed in Earth orbit with the proper heat shield if the heating problem cannot otherwise be solved. If this were done, an ideal structure for buoyant entry and heat protection seems to be the tension shell (ref 62:26-27). A tension shell is a body of revolution designed to have only tensile stresses under axisymmetric aerodynamic loadings (figures 12 & 13). The results of a study (ref 63:1.13) by M.S. Anderson indicates that this design of an entry vehicle concept leads to high drag and low weight, which is desirable for ballistic entry. This structural shape has 30% less structural weight than a sphere having the same base diameter and for large vehicles can lead to a major increase in payload (ref 62:26). The possibility of obtaining the advantages of this structural shape with a deployable airmatt system should be investigated.

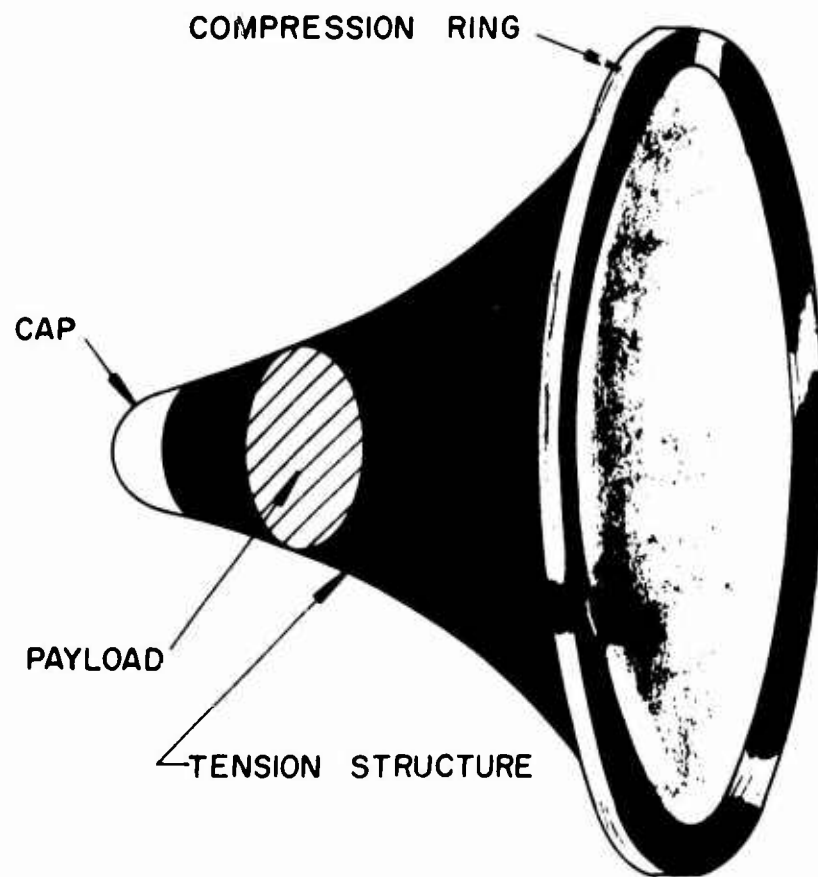
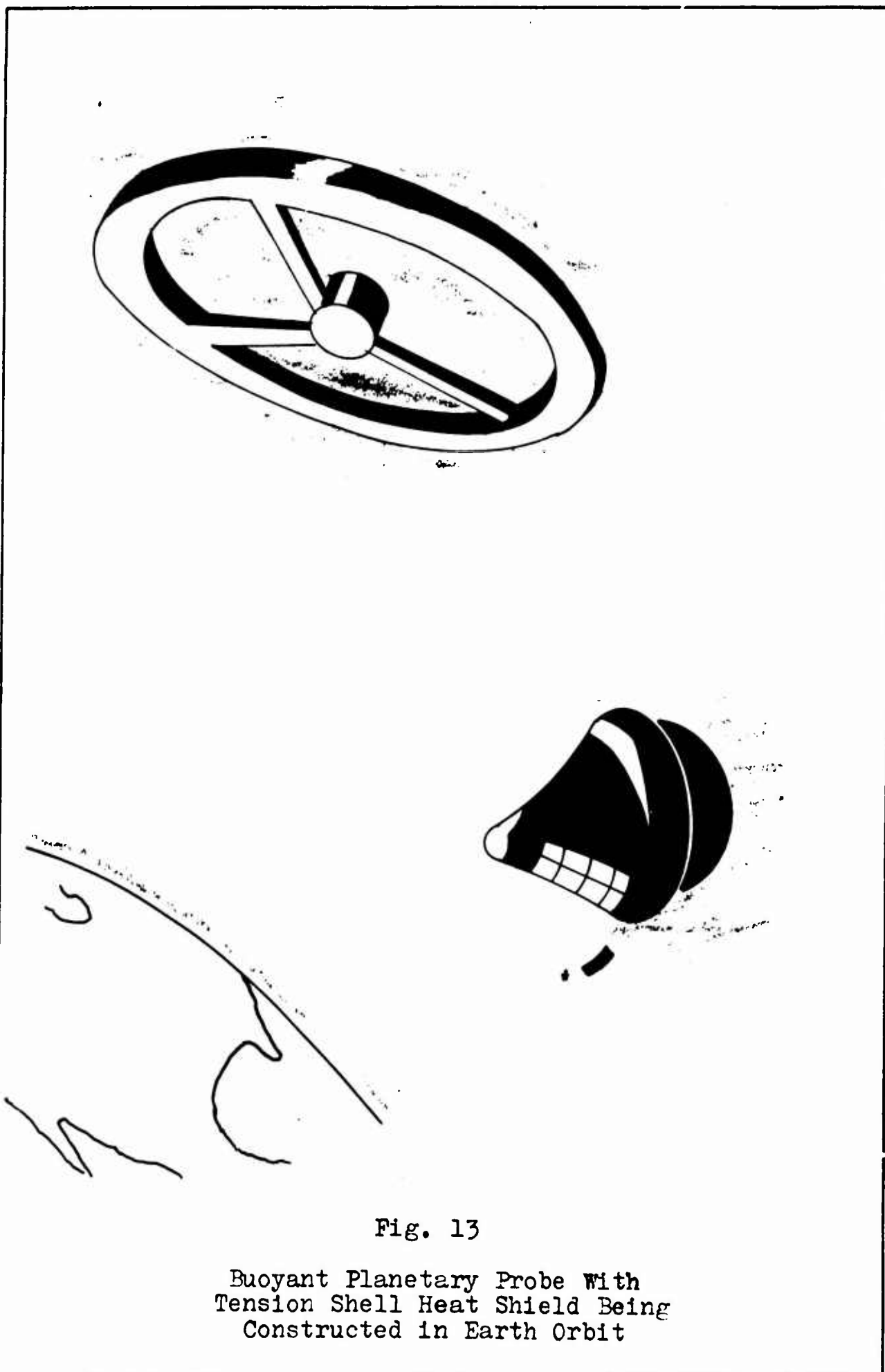


Fig. 12

A Tension Shell

( From ref 63 : 17 )



With a tension shell structure, direct entry from space into a planetary atmosphere is possible, eliminating the need for complicated maneuverings and retro-rocket braking.

### Spinning Spherical Entry Bodies

It was shown in the previous chapter that spherical spinning entry bodies have much reduced maximum temperatures. This has been thoroughly investigated in a study by H. Reismann (ref 63:151-159). Reismann's study concludes that

1. Maximum temperature alleviation occurs when the axis of rotation of the sphere is at right angles to the free-stream velocity.
2. Stagnation temperatures can be reduced by as much as 50% for low spin rates (about 1 rpm or greater).
3. Maximum temperature reduction occurs on the surface of the sphere.
4. The temperature gradient in the sphere is reduced by rotation, which decreases thermal stresses during entry.

### Optimum Compromise Between Minimum Retro-Rocket Braking and Buoyant Force Contribution

An examination of eq (85) shows that if the entry velocity is decreased (by using retro-rockets, for example) the buoyant force term could become noticeable. For example, if it is feasible that a reduction in velocity due to buoyant force compared to the non-buoyant case on

the order of 10% is possible. This would correspond to a decrease in the heating rate of about 25% for vertical entry. Gazley has pointed out (ref 17:25) the interesting fact that the heating rate during direct vertical entry of Mars is less than the circular orbit decay of a non-lifting body into Earth's atmosphere by an order of magnitude. Further, the heating during a Martian entry occurs at a higher altitude. This is due to the more gradual variation of density in the Martian atmosphere compared to Earth (ref 17:25).

Another method of increasing the effectiveness of the buoyant force term for direct entry into a planetary atmosphere is to decrease the velocity by successive grazing maneuvers into the atmosphere. This method was also described in Chapter II as a means of inserting the vehicle into a circular orbit around the planet. Although the required guidance accuracies are high and the complexities introduced are considerable, a vehicle may be made to enter a planetary atmosphere and emerge at a predetermined angle and velocity. The method, described by J. Warga and W.C. Hailey (ref 64:335-338), consists of maneuvering the vehicle while it is in the atmosphere by lift-drag ratio modulation. Moulin (ref 65:110-117) has described a method for optimizing the atmospheric braking maneuver by combining low thrust braking outside the atmosphere with drag braking inside the atmosphere. His analysis indicates that an optimum compromise may exist between rocket and atmospheric

braking when low thrust braking is used. Both the above methods would significantly reduce the weight of rocket motors and fuel which may otherwise be required.

It appears to be true, then, that there may be an optimum "trade-off" between atmospheric braking not requiring great accuracy, and low-thrust (e.g., electric propulsion) rocket propulsion not having great weight which would lower the entry velocity enough to make the buoyant term considerable. This may enable large savings in the weight of heat protection devices which may otherwise be required.

#### Configurations

Some possible configurations for a buoyant entry vehicle, based on the preceeding considerations, are shown in figure 14.

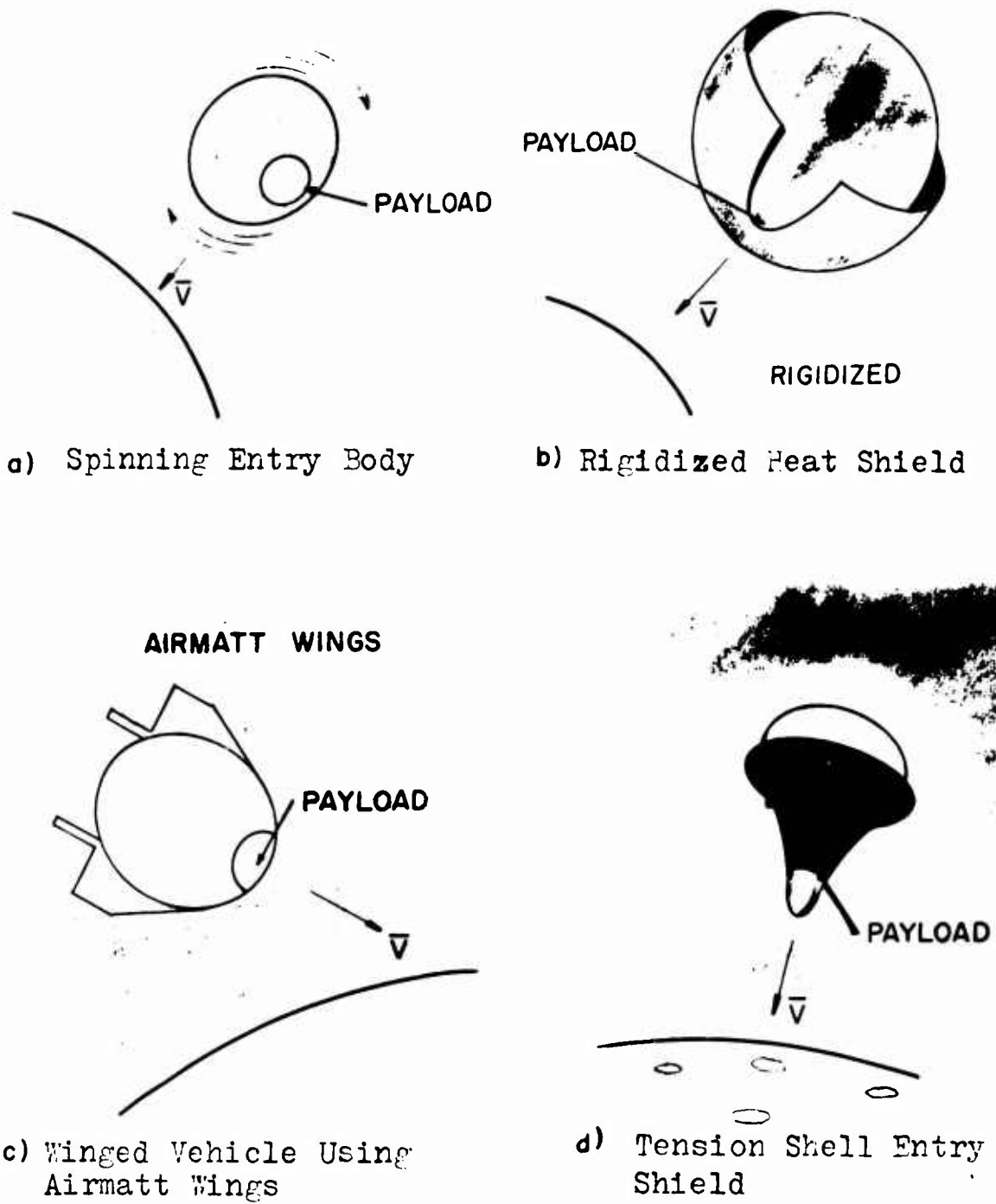


Fig. 14

Possible Buoyant Planetary Entry  
Vehicle Configurations



## V. Conclusions and Recommendations

### Conclusions

1. The effect of buoyancy per se on maximum deceleration, altitude of maximum deceleration, peak heating, and velocity for zero lift planetary entries is negligible. This is because peak heating and maximum deceleration occur at altitudes too high for buoyancy to have any effect. This is true even for very large buoyant cell diameters (above 500 ft.) and even if initial entry velocities are decreased.
2. The effect of buoyancy on velocity and, particularly maximum deceleration for small-angle gliding entries is small, but not entirely negligible. For example, the maximum deceleration for an equilibrium-glide trajectory is decreased by about 3.6% for Earth for a vehicle with a buoyant diameter of 200 ft. and a lift-drag ratio of 0.1. For Mars the maximum deceleration for this kind of entry is increased by 0.8% for a diameter of 300 ft. and a lift-drag ratio of 1.0. For Venus, the maximum deceleration is increased by 0.7% for diameters of 300 ft. and lift-drag ratios of 1.0. These percentage decreases are with respect to the value of maximum deceleration for non-buoyant entry.
3. Using the concept of the Douglas "drag cone", soft landings on Venus and Mars using balloons appears feasible. The technique would be to design the buoyant

volume to be large enough to decelerate the vehicle to hydrostatic equilibrium at a predetermined altitude above the planet. As the gas inside the buoyant cell cools, the capsule will descend slowly and should impact the ground with very low velocities. For Mars, the payloads would be quite small (on the order of 300-600 Mars pounds) for diameters of 250 ft. This figure is based on using light mylar films for the balloon skin, protected during entry by an airmatt drag cone which can be dropped away during the terminal descent. For Venus, this system should be able to deliver several thousands of pounds to the surface. It is realized that the penalty paid in the weight of heat shield is probably greater than that due to retrorockets with this system. But the important advantage of simplicity has been gained and the error margins greatly reduced.

4. The main advantage in the alleviation of entry heating by using a vehicle such as the one proposed is due to the increase in the parameter  $\frac{C_D S}{W}$ . If the materials are kept light and the diameter is large, entry  $\frac{C_D S}{W}$  values of 10 or greater should be possible. This would allow maximum heating and deceleration at higher altitudes and alleviate the heating problem somewhat.

5. For direct launches from Earth to Venus and Mars, shallow gliding or orbit-decay entries from circular speeds with some sort of heat shield protection, such as the airmatt drag cone or rigidized inverted umbrella would be necessary. With further increases in the state

of the art of expandable, highly heat-resistant airmatt or metal fabric materials, it may be expected that direct entries at parabolic speeds will become possible.

#### Recommendations for Further Study

During the course of this study several interesting problems and possibilities come to light which should be further investigated:

1. If a large buoyant sphere were spinning in the right direction on entry into a planetary atmosphere it would develop lift due to the Magnus effect. Lift has been shown by many authors to be a highly useful method for decreasing heating loads considerably. Therefore, this effect should be studied for the buoyant sphere or cylinder.

2. The mechanism of heat transfer through thin-walled organic sphere skins (such as polyethylene) by using the internal helium as a heat sink, combined with the mechanism of helium film cooling with regard to this problem should be investigated. This should include a method of controlling the amount of energy transfer into the buoyant cell.

3. The possibility of achieving a workable tension shell or similarly advantageous structure by using airmatt expandable techniques should be investigated.

4. The method of Linnell for computing vertical trajectories should be extended to include a buoyant force (ref 66 ).

# BIBLIOGRAPHY

1. National Aeronautics and Space Administration. "Summary Report, Future Programs Task Group" A Report of the National Aeronautics and Space Administration to the President. Washington, D.C., 1965.
2. Normyle, W.J. "Post Apollo Projects Detailed for Congress," Aviation Week, 82:12, 22 March 1965.
3. Koelle, H.H. "Manned Planetary Flight-Where Are We Today?", in Engineering Problems of Manned Interplanetary Exploration, New York: American Institute of Aeronautics and Astronautics, 1963.
4. Ehricke, K.A. Study of Interplanetary Missions to Mercury Through Saturn With Emphasis on Manned Missions to Venus and Mars 1973/82 Involving Capture. General Dynamics/Astronautics Report GD/A 63-0916. San Diego: 1963.
5. Associated Press. "Scientists Urge Venus Probes," Dayton Daily News, 16 January 1965.
6. Normyle, W.J. "Scientists Detail Mars Priority Argument," Aviation Week, 82:19, 10 May 1965.
7. National Academy of Sciences Space Science Board, "Biology and the Exploration of Mars", Astronautics And Aeronautics, 3:10, October 1965.
8. Stone, I. "Atmosphere Data to Alter Voyager Design," Aviation Week, 83:21, 22 November 1965.
9. Stone, I. "Mariner Data May Limit Voyager Payload", Aviation Week, 83:5, 2 August 1965.
10. NASA SP-56, ed. Dr. F.H. Quimby. Concepts for Detection of Extraterrestrial Life. Washington, D.C: National Aeronautics and Space Administration, 1964.
11. Jones, J. "Life on Venus? Not So Far-Fetched, Astronomers Say," Dayton Daily News, 23 January 1966.
12. Fink, D.E. "Manned Planetary Flights Studied in Detail", Aviation Week, 83:10, 6 September 1965.
13. Bilborn, T.W. "Balloons for Scientific Research," Astronautics and Aeronautics, 3:12, December 1965.

14. Hanel, R.A., et al. Experiments From a Small Probe Which Enters the Atmosphere of Mars. NASA TN-1899 Washington: National Aeronautics and Space Administration, 1963.
15. Hanel, R.A. Exploration of the Atmosphere of Venus by a Simple Capsule. NASA TN D-1909. Washington, National Aeronautics and Space Administration, 1964.
16. Loh, W.H.T. Dynamics and Thermodynamics of Planetary Entry. Englewood Cliffs, N.J.: Prentice Hall, Inc., 1963.
17. Gazley, Carl, Jr. Deceleration and Heating of a Body Entering a Planetary Atmosphere From Space. Rand Report P-955. Santa Monica, California: The Rand Corporation, 1957.
18. Gazley, Carl, Jr. The Penetration Of Planetary Atmospheres. Rand Report p-1322. Santa Monica, California: The Rand Corporation, 1958
19. Gazley, Carl, Jr. Atmospheric Entry. Rand Report P-2052. Santa Monica, California. The Rand Corporation 1960.
20. Duncan, Robert C. Dynamics of Atmospheric Entry. New York: McGraw-Hill Book Company, Inc., 1962.
21. Committee on Science and Astronautics. Inflatable Structures in Space. Hearing before the committee on Science and Astronautics, U.S. House of Representatives 87th Congress, 1st Session, 19 May 1961.
22. Ross, Jack H. "Flexible Fibrous Materials and Coatings for Expandable Reentry Systems," in Aerospace Expandable Structures - Conference Transactions, pp 74-94. Wright-Patterson Air Force Base, Ohio: Air Force Aero Propulsion and Flight Dynamics Laboratories, 1963.
23. Nebicker, F.R. "Expandable Drag Devices for Mach 10 Flight Regime", in Aerospace Expandable Structures - Conference Transactions, pp 501-510. Wright-Patterson Air Force Base, Ohio: Air Force Propulsion and Flight Dynamics Laboratories, 1963.
24. Chapman, D.R. An Approximate Analytical Method For Studying Entry Into Planetary Atmosphere. NACA Technical note 4276. Washington D.C: National Advisory Committee for Aeronautics, 1958.

25. Robinson, Alfred C., and A.J. Besonis. On the Problems of Reentry into the Earth's Atmosphere. WADC Technical Report 58-408. Wright-Patterson Air Force Base, Ohio: Wright Air Development Center, 1958.
26. Lees, Lester, et al. "Use of Aerodynamic Lift During Entry Into the Earth's Atmosphere". ARS Journal, 29: 633-641 (September 1959).
27. Allen, H.J., and A.J. Eggers, Jr. A Study of the Motion and Aerodynamic Heating of Ballistic Missiles Entering the Earth's Atmosphere at High Supersonic Speeds. NACA Technical Report 1381. Washington, D.C. National Advisory Committee for Aeronautics, 1958.
28. Eggers, A.J., et al. A Comparative Analysis of the Performance of Long-Range Hypervelocity Vehicles. NACA Technical Report 1382. Washington D.C. National Advisory Committee for Aeronautics, 1958.
29. Nebiker, F.R. "Inflatable Decelerator Developed for Re-entering Space Capsules", in SAE Journal 71:101, 1963.
30. Foerster, A.F., "Theoretical and Experimental Investigation of Metal Fabric Expandable Structures for Aerospace Applications" in Aerospace Expandable Structures-Conference Transactions, pp 95-117, Wright-Patterson Air Force Base, Ohio, 1963.
31. Eskinazi, Salamon. Principles of Fluid Mechanics. Boston: Allyn and Bacon, Inc. 1962
32. Brenkert, Karl, Jr. Elementary Theoretical Fluid Mechanics. New York: John Wiley & Sons, Inc., 1960
33. Wolaver, L.E. Analytical Techniques in Astrodynamics-An Introduction. Air Force Institute of Technology lecture notes for course MECH 325. Wright-Patterson Air Force Base, Ohio: Aerospace Research Laboratories, 1965.
34. Patterson, Gordon H. "A Synthetic View of the Mechanics of Rarefied Gases", (AIAA Paper No. 65-224), in AIAA 2nd Aerospace Sciences Meeting, 25-27 Jan. 65. New York: American Institute of Aeronautics and Astronautics, 1965.
35. Dommasch, D.O., et al. Airplane Aerodynamics. New York: Pitman Publishing Corporation, 1951.
36. Riley, F.E., and J.D. Sailor. Space Systems Engineering. New York: McGraw Hill Book Company, Inc., 1962

37. Katz, G.D., and J.C. McMullen. "Entry Vehicles for Unmanned Planetary Exploration" in AIAA Entry Technology Conference. New York, American Institute of Aeronautics and Astronautics, 1964.
38. Ohring, George, et al. Planetary Meteorology. NASA Cr-280. Washington, D.C.: National Aeronautics and Space Administration, 1965.
39. Graham, T.L. and R.G. Spain. Rigidization of Expandable Structures Via Gas Catalysis, in Aerospace Expandable Structures-Conference Transactions, Wright-Patterson Air Force Base, Ohio: Air Force Aero Propulsion and Flight Dynamics Laboratories, 1963.
40. Schwartz, S. et al. "Ultraviolet and Heat Rigidization of Inflatable Space Structures" in Aerospace Expandable Structures-Conference Proceedings. Wright-Patterson Air Force Base, Ohio. Air Force Aero Propulsion and Flight Dynamics Laboratories, 1963.
41. Phillips, R.L., and C.B. Cohen. "Use of Drag Modulation to reduce Deceleration During Atmospheric Entry, in ARS Journal, Vol 29. No. 6. June 1956.
42. Hayes, J.E. and W.E. Vander Velde. "Satellite Landing Control System Using Drag Modulation". in ARS Journal May, 1962, pg 722.
43. Wang, K., and L. Ting. "An Approximate Analytic Solution of Reentry Trajectory With Aerodynamic Forces" in ARS Journal, pp 565-566. Vol 30, June 1960.
44. Burington, R.S. Handbook of Mathematical Tables and Formulas, New York: McGraw Hill Book Company, 1961.
45. Coming, G. Aerospace Vehicle Design. Published privately by the author at Box 14, College Park, Maryland, 1964.
46. Aller, Robert O. Effect of the Earth's Shape on Glide Trajectories. Unpublished Research Study, 1960, Ann Arbor, Michigan, University of Michigan.
47. Moe, Mildred M. "An Approximation to the Re-Entry Trajectory" in ARS Journal vol 30, No. 1, pp 50-53, January, 1960.

48. Katzen, E.D. "Terminal Phase of Satellite Entry Into the Earth's Atmosphere" in ARS Journal, pp 147-148, vol 29, February 1959.
49. Gazley, Carl, Jr. and D.J. Masson. "A Recoverable Scientific Satellite. Rand REport RM-1844. Santa Monica, California: The Rand Corporation, 1956.
50. Schlichting, Hermann. Boundary Layer Theory. New York: McGraw Hill Book Company, 1960.
51. Binder, R.C. Fluid Mechanics. Englewood-Cliffs, N.J.: Prentice-Hall, Inc., 1955.
52. Scoggins, James R. "Aerodynamics of Spherical Balloon Wind Sensors" in Journal of Geographical Research, Vol 69, No.4, February, 1964.
53. Reed, W.H., III. Dynamic Response of Rising and Falling Balloon Wind Sensors With Application to Estimates of Wind Loads on Launch Vehicles. NASA TN D-1821. Washington D.C. National Aeronautics and Space Administration, October 1963.
54. Allen, H.J., et al. Aerodynamic Heating of Conical Entry Vehicles at Speeds in Excess of Earth Parabolic Speed. NASA TR R-185. Washington. D.C. National Aeronautics and Apace Administration,,1963.
55. Dannenberg, Robert E. Helium Film Cooling on a Hemisphere at a Mach Number of 10. NASA TN-1550. Washington, D.C. National Aeronautics and Space Administration, 1962.
56. Air Force Aero Propulsion and Flight Dynamics Laboratories. Aerospace Expandable Structures-Conference Transactions. A conference held 23-25 October 1963 at NCR Sugar Camp, Dayton, Ohio. Wright-Patterson AFB, Ohio, 1963.
57. Clemmons, Dewey L., Jr. The Echo I Inflation System. NASA TN D-2194. Washington, D.C. National Aeronautics and Space Administration, 1964
58. Fichter, W.B., et al. Buckling of the Echo A-12 Passive Communications Satellites NASA TN D-2353. Washington D.C., National Aeronautics and Space Administration, 1964
59. Forbes, F.W. "Expandable Structures" in Space Aeronautics, 42:7, December 1964.



60. Demele, F.A. A Study of the Convective and Radiative Heating of Shapes Entering the Atmospheres of Venus and Mars at Superorbital Speeds. NASA TN D-2064. Washington, D.C: National Aeronautics and Space Administration, 1963.
61. Katz, G.D., and J.C. McMullen. "Entry Vehicles for Unmanned Planetary Exploration", in AIAA Entry Technology Conference, AIAA pub. CP-9. New York, American Institute of Aeronautics and Astronautics, 1964.
62. Roberts, L. "Entry Into Planetary Atmospheres", in Astronautics and Aeronautics, 2:10, October 1964.
63. Reismann, Herbert. "Temperature Distribution in a Spinning Sphere During Atmospheric Entry", in Journal of Aerospace Sciences, 29:2 February 1962.
64. Warga, J. and W.C. Hailey. "Determination of Extreme Entry Angles into a Planetary Atmosphere", in AIAA Journal, 2:2, February, 1964.
65. Moulin, L. "Recovery of Interplanetary Vehicles by Low-Thrust Braking Outside the Atmosphere", in Astronautica Acta, 11:2, March-April, 1965.
66. Linnell, R.D. "Vertical Reentry into the Earth's Atmosphere for Both Light and Heavy Bodies", in Jet Propulsion, 28:5, May, 1958

## Appendix A

Characteristics of Venus and Mars

The atmospheric and other characteristics of Mars and Venus as used in this study are presented below.

Mars

$$g_0 = 12.3 \text{ ft/sec}^2 \quad R_p = 1.1 \times 10^7 \text{ ft.}$$

$$\rho_0 = 2.56 \times 10^{-5} \text{ SLUGS/FT}^3 \quad \beta = 2.15 \times 10^{-5} \text{ ft}^{-1}$$

Venus

$$g_0 = 28.3 \text{ ft/sec}^2 \quad R_p = 2.03 \times 10^7 \text{ ft.}$$

$$\rho_0 = 5.82 \times 10^{-2} \text{ SLUGS/FT}^3 \quad \beta = 4.9 \times 10^{-5} \text{ ft}^{-1}$$

## Appendix B

Assumption of Negligible Terms

If eq (105) is multiplied out, one obtains

$$\gamma_E + 2\gamma_E \ln\left(\frac{V}{V_E}\right) + \ln\left(\frac{V}{V_E}\right) \frac{W_V}{W_D} \frac{1}{V_E^2}$$

$$= -\frac{L}{D} \ln\left(\frac{V}{V_E}\right) - \frac{L}{D} \left[ \ln\left(\frac{V}{V_E}\right) \right]^2 + 2\gamma_E W_D$$

The quantity  $\frac{1}{V_E^2} \frac{W_V}{W_D}$ , from the definitions for  $W_D$  and  $W_V$ , is equal to

$$\frac{2 g_0 d}{3.3 V_E^2}$$

Since the descent is from circular orbit

$$V_E^2 = g_0 R_P$$

Therefore

$$\frac{1}{V_E^2} \frac{W_V}{W_D} = \frac{2d}{3.3 R_P}$$

The radius of the planets Mars and Venus are on the order of  $10^7$  ft.

Even for very large buoyant volume diameters of, say, 500 ft, the

quantity  $\frac{1}{V_E^2} \frac{W_V}{W_D}$  is seen to be much less than one. The quantities  $\gamma_E$  and  $\ln\left(\frac{V}{V_E}\right)$  are on the order of 0.04 radians and 0.2-0.3, respectively. The quantity  $\frac{L}{D}$  varies from about 0.1 to 3.0.

The quantity  $y_E$  is defined by

$$y_E = e^{-\beta h_E}$$

where  $\beta h_E$  is on the order of 8-10. The quantity  $W_D$  is defined by

$$W_D = \frac{C_D S}{m} \frac{P_0}{2g_0}$$

The quantity  $\frac{C_D S}{m}$  is taken to vary through the wide range of values 0.1 to 50. Thus,  $W_D$  is seen to be much less than one for Mars and on the order of 0.05 for Venus for the large  $\frac{C_D S}{m}$  value of 50 (a normal value of  $\frac{C_D S}{m}$  would be 5 or 10). Since the quantity  $y_E$  is already on the order of  $10^{-3}$ , the quantity  $2W_D y_E$  is seen to be negligible compared with  $\gamma_E$ ,  $\gamma_E \ln\left(\frac{V}{V_E}\right)$ , or

$$\frac{L}{D} \left[ \ln\left(\frac{V}{V_E}\right) \right]^2.$$

## VITA

[PII Redacted]

Reginangelo A. DiPilla was born on [REDACTED], the son of Antonio DiPilla and Filomena Salzano DiPilla. He attended Xavier University, in Cincinnati, and St. Louis University where he graduated with the degree of Bachelor of Science and a commission as Second Lieutenant in the USAF in July 1958. He entered active duty in August 1958, attending a course in communications operations at Scott AFB, Illinois. He was subsequently assigned to Aviano AB, Italy, where he served for three years as a communications officer. Before coming to AFIT, he was assigned to one of four world-wide based "Talking Bird" tactical communications aircraft.

Permanent home address: [REDACTED]  
[REDACTED]

[PII Redacted]

This thesis was typed by Mrs. Nancy A. Reif